Design and Development of A Novel Slurry Pump Using Transmission Roller

by

Hanbo Li

B.Eng., Zhejiang University, 2012

Thesis Submitted in Partial Fulfillment of the
Requirements for the Degree of
Master of Applied Science

in the
School of Mechatronic Systems Engineering
Faculty of Applied Sciences

SIMON FRASER UNIVERSITY

Summer 2015

Approval

Name:	**Hanbo Li**
Degree:	**Master of Applied Science**
Title:	***Design and Development of A Novel Slurry Pump Using Transmission Roller***
Examining Committee:	**Chair:** Flavio Firmani Lecturer

Siamak Arzanpour
Co-Supervisor
Associate Professor

Gary Wang
Co-Supervisor
Professor

Krishna Vijayaraghavan
Internal Examiner
Assistant Professor

Date Defended/Approved: August 12, 2015

Abstract

The oil and gas industry needs a simple and compact pump that could deal with slurry and other highly viscous or erosive fluid. The pump should also be able to fit in limited space of a borehole while maintaining comparable or higher efficiency than the current applications. Inspired by the algebraic screw, a new design of power transmission device, named as Transmission Roller, is introduced in this work and incorporated into a diaphragm pump. This mechanism converts rotary motion into linear motion and shows promises of high efficiency with its compact structure. Similar mechanisms have never been used in a hydraulic application before. A pump prototype utilizing the Transmission Roller is built and tested with water to prove its functionality. The transmission efficiency of the transmission roller prototype is 73.6%. The Transmission Roller efficiency for the final production pump design is expected to be 96.3%, higher than other designs of the same kind.

Keywords: slurry pump; diaphragm pump; power transmission device; prototype building

Acknowledgements

Research is a tough but rewarding process. I would like to express my gratitude to my dear supervisors Dr. Gary Wang and Dr. Siamak Arzanpour, without whom I cannot finish this adventurous long journey.

I would also like to thank my colleagues at SFU for their support and inspiration. In particular, I would like to thank Shahab Azimi who has given me countless advice and help to the process of pump design and prototype building. Also, I would like to thank Mazen Kawam for his help in CAD drawings, George Cheng and Yu Guo their help in ANSYS.

I would also like to acknowledgement Toyo Pumps and Mitacs for providing this opportunity to gain invaluable industrial experience.

I also wish to show my appreciation to my friends who have encouraged me during my most difficult times.

Last but most importantly, I extend gratitude to my parents, Hui and Yu, for the unbelievable amount of support and understanding.

Table of Contents

List of Tables

List of Figures

List of Acronyms

DC	Direct Current
EAP	Electroactive Polymer
GDP	Griffis-Duffy Platform
GPM	Gallon Per Minute
NPSH	Net Positive Suction Head
NPSHR	Net Positive Suction Head Required
NPT	National Pipe Thread
PDP	Positive displacement pump
PI	Physik Instrumente
PTFE	Polytetrafluoroethylene
SS	Stainless Steel
UST	Unified Thread Standard

Glossary

Algebraic Screw	Definition goes here, see example and notes below
Slurry	A mixture of solids and liquids
Bench Power Supply	A stand-alone desktop unit used in applications such as circuit test and development

List of Symbols

Chap.1

δ_0	Separation distance between the two manipulators of the algebraic screw at static equilibrium point
θ_0	Rotation angle of the algebraic screw at static equilibrium point
δ	Separation distance between the two manipulators of the algebraic screw
θ	Rotation angle of the algebraic screw

Chap.2

D_t	Diameter of the plunger for the track part
F_{max}	Blocking force of a piezoelectric actuator
P_A	Maximum power of a piezoelectric actuator
f_0	Resonant frequency without load of a piezoelectric actuator
$f_0{}'$	Resonant frequency with load of a piezoelectric actuator
k_A	Stiffness of a piezoelectric actuator
m_{eff}	Effective mass of a piezoelectric actuator
p_a	Maximum pressure generated for the diaphragm pump
$p_{in}{}'$	Required pump input pressure for piezoelectric actuator assessment
$p_{out}{}'$	Required pump output Pressure for piezoelectric actuator assessment
ΔL_0	Nominal displacement of a piezoelectric actuator
ΔL	Displacement of a piezoelectric actuator
h'	Pump head for piezoelectric actuator assessment
Q'	Minimum pump capacity for piezoelectric actuator assessment
Z'	Pump body length for piezoelectric actuator assessment
d'	Maximum pump diameter for piezoelectric actuator assessment
g	Gravity of earth
i	Number of rounds that the bearing group is going through around the plunger
l	Amplitude of the track curve
l'	Amplitude of the tracks for transmission roller II
n	Pump speed
t	Time
x	x coordinate for bearing 1

y	y coordinate for bearing 1
z	Displacement of the plunger
ρ	Density of the transferred fluid
ω	Rotary speed of the motor
$P_{min}{}'$	Minimum power required from the actuator

Chap.3

Q_i	Ideal pump flow rate
D	Diameter of the plunger

Chap.4

F_f	Friction force exerted by the track onto the bearing
F_{fld}	Force applied on the fluid by the transmission roller
F_{ld}	Load force applied on the transmission roller
F_p	Normal force exerted by the track onto the bearing
P_{mot}	Power of the motor
W_f	Friction loss of the transmission roller over one pump cycle
W_{mot}	Power provided by the motor over one pump cycle
a_f	Acceleration of transferred fluid
η_t	Transmission efficiency of the transmission roller
θ_t	Gradient angle of the tangent line of the track curve
τ_d	Average decelerating torque provided through F_p and F_f
τ_{mot}	Torque provided by the motor to the revolver
A	Constant in the expression of F_p
L	Height of the pump chamber when the plunger is in the middle of its stroke
T	Time for one pump cycle
m	Mass of the fluid in the pump chamber
μ	Coefficient of friction between the bearing and the plunger track

Chap.5

$\mathrm{D_v}$	Diameter of the check valve at the outlet
A_r	Area of the horizontal cross section of the outlet reservoir
P_W	Pump prototype output power

Z_{in}	Elevation head of the inlet
Z_{out}	Elevation head of the outlet
p_H	Total differential pressure between the inlet and outlet
p_{in}	Total suction pressure
p_{out}	Total discharge pressure
v_{in}	Flow velocity at the inlet
v_{out}	Flow velocity at the outlet
η_m	Efficiency of the motor
Δh	Water level increase in the outlet reservoir during the test
Δt	Total time for testing
I	Current provided by the power source
N	Number of pump cycles completed within the testing time period
Q	Pump prototype capacity
U	Voltage provided by the power source
η	Overall pump efficiency

Chapter 1.
Introduction

A slurry is a mixture of solid particles in water or other fluid, the mixture being of such a consistency that it can be pumped like a liquid [1]. A slurry pump is a type of pump that pumps slurry. Majority of slurry pumps are centrifugal pumps in the industry where pressure is generated by a rotating impeller, which often leads to a common misconception that all slurry pumps are centrifugal. For centrifugal slurry pumps, wear is the most significant plague to performance because the solid particles are in contact with the walls of the pump components [2]. In fact, positive displacement slurry pumps are also widely used, such as lobe pumps, peristaltic pumps and piston diaphragm pumps. One of the most ancient pumping systems in existence is the animal blood-circulating system, where the heart circulates a slurry of blood corpuscles in the serum through a complex pipeline, the veins. Lobe pumps and peristaltic slurry pumps are used in a variety of industries including pulp and paper, chemical and biotechnical industries. Piston diaphragm pumps are usually used to deal with slurries of high abrasivity. Unlike centrifugal pumps, diaphragm pumps protect the piston, liners, and plungers against abrasive slurry. However, no design has ever offered protection for liquid-end valves of a pump.

Slurry is often highly abrasive or viscous and the technology for pumping highly viscous or abrasive materials is highly needed in many industries, such as oil and coal slurry extraction, viscous chemical processing, sewage and sludge processing, and food processing. Especially in the oil and gas industry, production of heavy and extra-heavy crude oil involves the handling of fluid of very high viscosity and high gas void fraction, and mixtures of crude oil, gas, water, and sand [3]. Take the heavy and extra-heavy crude oil extraction as an example, when the hydrocarbon formation pressure is insufficient to force the oil to the surface, it must be pumped to the surface. Subsurface reciprocating pumps are often used in this service. A borehole is often drilled for this

application to locate the subsurface pump. A borehole is a narrow shaft bored in the ground, either vertically or horizontally. It may be constructed for many different purposes, including the extraction of water, petroleum or natural gas as part of a geotechnical investigation, environmental site assessment, mineral exploration, temperature measurement or as a pilot hole for installing piers or underground utilities [4]. The depth of a borehole ranges from 150 to 1000 ft and the diameter is usually around 3.5", which means conventional pumps with their huge power transmission systems wouldn't fit in this limited narrow space.

Other than the need to handle highly viscous and abrasive materials and the highly constraint space for equipment, the process of designing an appropriate pumping system is made even trickier by other factors. Chemical incompatibility with gases and liquid produced, the temperature of material handled down the well and the high differential pressure applied to pumps during operation affect their running life and reduce their volumetric and torque efficiency, resulting in increased operational cost. Currently subsurface reciprocating pumps used in some wells are driven hydraulically by power pumps installed at a ground-level near the well. A complex system like this also incurs high maintenance cost. A simpler design with a longer life span will certainly help decreasing the high maintenance cost with fewer parts and more compact structure. It has come to a stage for pump technologies where reducing operational and maintenance cost is the key to improvement and the crucial need from industry. This is because after the costs of operating the pump outweigh the revenue created, the wells are abandoned which left huge reserves behind. The amount of the unexploited reserves from these tired wells is as much as 1/3 of the entire North American known reserves. That's why a simple design is needed which requires less maintenance cost.

1.1. Motivation

Various pump manufacturers sell pumps for the purposes stated above. The available pumps could be categorized mainly in two kinds: multistage centrifugal pumps and positive displacement pumps.

A multistage centrifugal pump, which contains two or more impellers are usually used for deep well applications. The purpose of using a multistage pump is to reach higher output pressure if impellers are connected in series. However, lifetime for a multistage pump is short because of this large pressure. Blades of the impellers are always in contact with slurry so they are constantly withstanding the high output pressure generated by the pump. When the fluid is corrosive or erosive, it causes more wear on the blades which shortens its lifetime.

Different from multistage centrifugal pumps, positive displacement pumps that are used for this purpose separate slurry from its core pump components, thus having the features of low maintenance and longer life span compared with multistage centrifugal pumps. However, most positive displacement pumps come with complex and huge power transmission systems, such as sliding crank, cam shaft or gear transmission systems. These traditional systems are large and have low efficiency. Some positive displacement pumps are driven hydraulically by power pumps installed at a ground-level near the well, in which case the maintenance cost is very high because of the complex structure of the system and its large number of components that need to be maintained regularly.

The available pumps for deep well slurry applications, as explained above, are either unreliable with short life time, or too large, complex, and expensive. There is a need for a compact, rugged industrial pump that can reliably pump abrasive materials such as slurries or sand-contaminated crude oil from a deep well.

Toyo Pumps is a company located in Vancouver that manufactures slurry pumps. It is also to their interest to find a design which could withstand large pressure for deep wells and could fit in a borehole of 3.5”. Their requirements of specifications are, 1000 psi output pressure, 0-50 Hz frequency, -10°C to 50°C temperature variation, 1-5 year operating life cycle, 50~500 GPM flow rate, low manufacturing cost, comparable or higher overall pump efficiency than similar industrial pumps, with a dimensional constraint of a device diameter less than 3.5”. The body length of the pump could be 35”.

This thesis proposed a compact pump design for a deep well application which uses a novel mechanism, named as transmission roller, as a power transmission device

with high efficiency. The design of the transmission roller is inspired by the use of highly efficient algebraic screw for vehicular suspension systems. This algebraic screw or other similar mechanisms have not been used in hydraulic pumps before. Some of the specifications from Toyo pumps are used and considered as a common market benchmark for pumps for this application. However, the purpose of this thesis is not to meet all the requirements from Toyo Pumps.

1.2. Background

Before we go further in this topic, some background information about pumps and a literature review of related topics are presented in this section.

Looking back on the research and development of pump technologies, there are at least two surges in the 20th century [5]. The first surge happened in the first half of the century when infrastructure of advanced mechanical equipment was needed globally. In this period, a group of outstanding pump engineers and researchers made great contributions towards the knowledge and design of the pumps. Den Hartog showed in 1929 that pressure fluctuations in the penstock may become very large when the pressure waves reach the volute end in the same phase [6]. Fisher and Thomas reported in 1932 their observation of rotating stall and backflow in an impeller as they reduced the flow rate toward shutoff [7]. Knapp reported in 1948 that cavitation damage increases with the sixth power of velocity [8]. Blom described in 1950 his design of the Grand Coulee irrigation pumps with their 13 ft diameter impellers and over 90 percent efficiency [9]. Stahl and Stepanoff enunciated the thermodynamic effect on cavitation in 1956, demonstrating that NPSHR is reduced when pumping fluids with more favorable vaporization characteristics [10]. Net positive suction head required (NPSHR) is the minimum pressure required at the suction of the pump to keep the pump from cavitating. The first surge is obviously spurred by the technology needs of world wars and post war infrastructure development. But soon after that, there came a low period regarding pump research and development until the space race began between different countries.

The second surge also made distinguished contribution to pump technologies, including the 53,000 hp (40 MW) package that combined the oxygen and RP1 (kerosene)

pumps for each of the five engines of the Saturn V moon rocket's first stage, and the high-energy 28,000 hp (21 MW) oxygen pump and 77,000 hp (57 MW) hydrogen pump on each of the three space shuttle main liquid-propellant rocket engines. Most of the space technology R&D was carried out by NASA and its contractors, and academic institutions. Actual hydrodynamic pumps are designed by manufacturers. Furst presented design of the space shuttle pumps for Rocketdyne in 1978 [11]. In more recent years, there has been less emphasis on the R&D itself and more on various applications of pumps due to the massive global consolidation throughout the industry.

In the pump market today there are basically two types of pumps: centrifugal pumps and positive displacement pumps (PDPs). There are several billion of each type in use [12]. A positive displacement pump, such as a diaphragm pump, is very different from centrifugal pumps. Positive displacement pumps force the fluid along by volume changes, while centrifugal pumps add momentum to the fluid by rotating blades or vanes. Centrifugal pumps generate pressure by rotating blades, while positive displacement pumps produce a flow of fluid. Resistance to this flow is produced by downstream process or piping system, thereby pressure is generated in the piping system and in the discharge portion of the pump. Therefore, flow rate does not have much impact on the output pressure of a positive displacement pump. Because of its special way of pumping fluid, positive displacement pumps can handle highly viscous fluid much better than centrifugal pumps.

Positive displacement pumps (PDPs) have been used in various industries for over 2000 years [13]. The development of the very early power-driven PDP is attributed to Ctesibius of Alexandria, Egypt about 150 B.C. [14], about 100 years after the screw pump was invented by Archimedes. One of the first applications of steam power to drive a pump was introduced in 1711 which connects a conventional reciprocating water well pump to a steam-driven piston. In recent years, centrifugal pumps gradually gain more popularity than PDPs. PDPs are still being used in various industries. For example, in the petroleum industry, reciprocating pumps are being used in pumping mud during the drilling of an oil or gas well. In the automobile industry, they are being used in pumping of the gasoline into the carburetor in the automobile engine. In the chemical industry, they are being used in fertilizer plants, detergent production, and plastic production.

PDPs are also used to deal with slurries. One of the reasons that a diaphragm pump is chosen for this project is its capability of dealing with slurries, which will be further illustrated later in this chapter.

1.2.1. Slurry Pumps

As introduced at the beginning of this chapter, slurry is a mixture of solid particles in water or other liquid which could be pumped like a liquid [15]. Hardness and sharpness of the particles in the slurry decide its abrasivity. Unlike erosion, mechanical abrasion is unpredictable and few data has been collected in this area. ASTM Standard G75.82, known as the Miller Number, has been developed as a standard method of measuring abrasivity of slurries [16]. The primary purpose is to rank the abrasivity of slurries in terms of the wear of a standard reference material. The wear damage is worse as the Miller Number gets higher.

Centrifugal pumps have been used to transfer slurry, but they have been used where low heads are required, typically up to 100 psi or so. Abrasive liquids have a deteriorating effect on the impellers and the casings through which they flow, as a result of the erosion caused by the liquid and the suspended particles. The advantage of centrifugal slurry pumps is that they have a high capacity of a relatively low capital cost and usually require relatively little space. One of the disadvantages lies in the flow rate pressure performance relationship. Centrifugal pumps generate pressure by rotating blades. A centrifugal pump provides increased pressure at the expense of reduced flow rate. This feature tends to work against the slurry applications. If an increase in pressure is incurred by flow restriction in the pipeline, a desirable characteristic of a slurry pump should be able to develop increased pressure to overcome that restriction. For centrifugal pumps, a lower flow rate is needed to generate that increased pressure. With the reduced flow rate, the fluid velocity might be inadequate to hold the material in suspension and keep it flowing in the pipe.

Positive displacement pumps have also been used to pump slurry. PDPs have the desirable characteristic of maintaining high volumetric efficiency at any desired flow rate. PDPs maintain a constant flow rate regardless of pressure, thereby tending to

“purge” any plugging effect. PDPs usually have longer lifetime than centrifugal slurry pumps. Unlike other designs, PDPs don’t require complete dismantling and overhaul when parts are worn out. They are designed so that liquid end parts that are subject to the deteriorating effects of slurries can be easily replaced. PDPs have been used for years in the oil well drilling industry for pressures up to 4000 psi or more. One of the disadvantages is that PDPs usually take large space and it is a challenge to put them in a borehole.

1.2.2. Diaphragm Pumps

Diaphragm pump is a type of positive displacement pumps which is often used to pump slurry or other erosive or highly viscous fluid. It uses reciprocating action of a rubber, thermoplastic or Teflon diaphragm and suitable valves on both ends to pump fluid. Diaphragm pump is widely used for pumping chemicals, dry powders, food additives, glues, paints, pharmaceutical products, slurries, tailings, and wastewater. With the development in engineering concept, metals and elastomers, there is an increasing interest in diaphragm pumps for the pumping of abrasive slurries, particularly with slurries of abrasivity above Miller number 50 [15]. A traditional diaphragm pump design is illustrated in Figure 1-1 and Figure 1-2.

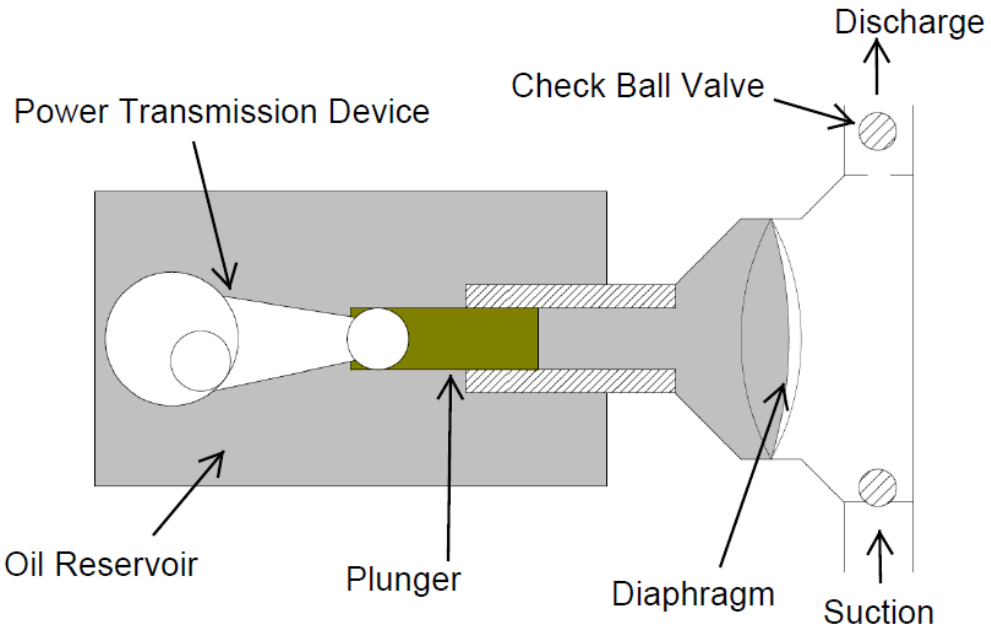

Figure 1-1. Diaphragm Pump during Discharge Stroke

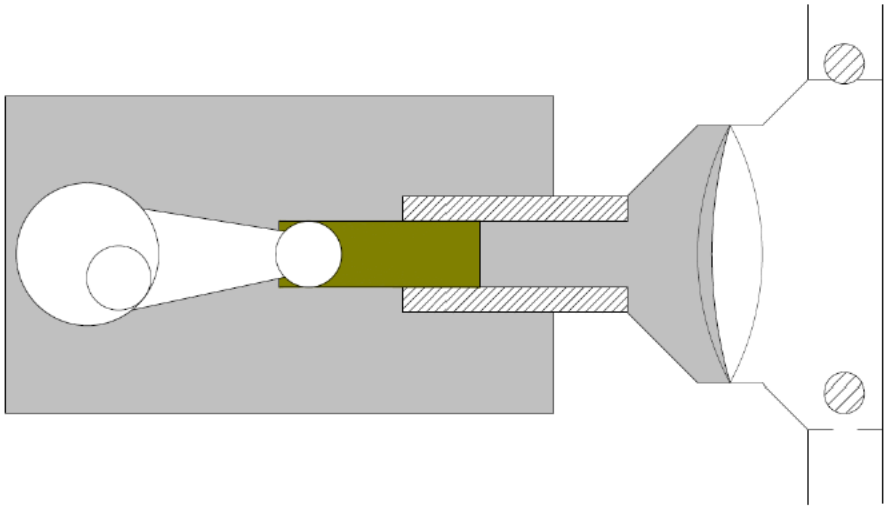

Figure 1-2. Diaphragm Pump during Suction Stroke

A check valve is a valve that allows fluid to flow through it in only one direction. A ball check valve is a check valve in which the closing member, the movable part to block the flow, is a spherical ball. A plunger reciprocating at a fixed stroke displaces a fixed volume of hydraulic fluid, which actuates a flexible diaphragm to create a pumping

action. In operation as shown in Figure 1-1, the plunger pushes forward and thus pressurizes the oil between the plunger and the diaphragm. That pressure is imposed on the flexible diaphragm that moves and displaces the discharge ball check valve while the suction ball check valve remains closed. Thus, this stroke is called discharge stroke.

On the suction stroke, the pump plunger pulls oil out of the diaphragm cavity, which moves the flexible diaphragm toward the plunger. The internal pressure drops and thus opens the suction ball check valve and closes the discharge ball check valve. Fluid is pulled in through the suction ball check valve.

Because of its unique design, diaphragm pumps have many advantages over centrifugal pumps. One distinguishing feature of diaphragm pump is that the absence of seals and packing, which makes it a popular choice for applications requiring zero leakage [17]. Another feature is its ability to handle highly viscous and abrasive materials. However, the large volume of its power transmission device makes it impossible to be applied directly to borehole applications illustrated at the beginning of this chapter.

Different solutions have been suggested to make up for this disadvantage of diaphragm pumps in the thesis. Using piezoelectric material as its actuation has also been assessed as a possible solution.

1.2.3. Piezoelectricity

Piezoelectric material has been considered for pump actuation to achieve a compact design of diaphragm pump. However, according to the assessment its generated power is nowhere near the requirements from Toyo Pumps, which are used as a benchmark for deep oil pump applications. A literature review of piezoelectricity is presented in this section.

The word "piezo" is derived from the Greek word for pressure. Pierre and Jaques Curie first discovered the phenomenon of piezoelectricity in 1880 (Piezo Systems, Inc. 2002) [18]. They called this phenomenon the "piezoelectric effect". Later they noticed that electrical fields can deform piezoelectric materials. This effect is called the "inverse piezoelectric effect". Development in the following years involves various kinds of

piezoelectric material being used in different applications of various fields, including underwater entities detecting systems, phonograph cartridges, ignition systems, and microphones [19].

Pressure generates electric charges on the surface of piezoelectric materials. This direct piezoelectric effect converts mechanical energy into electrical energy. Vice versa, the inverse piezoelectric effect causes a change in length in this type of materials when an electrical voltage is applied. This actuator effect converts electrical energy into mechanical energy, as shown in Figure 1-3.

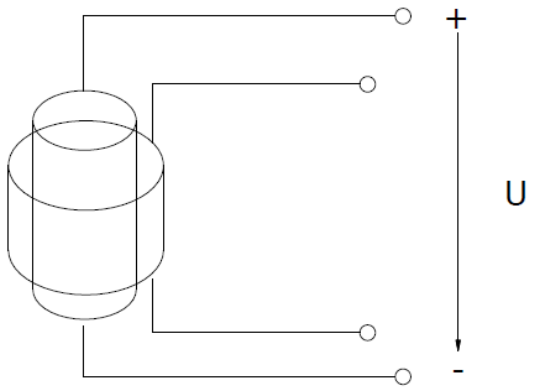

Figure 1-3. Piezoelectric Material under Electric Voltage

Actuators are one important application for piezoelectric material for precision positioning and vibration suppression [20]. Some reliable and low cost piezoelectric actuators have been developed, including Unimorphs, Bimorphs, Rainbows [21], Thunder [22] [23], and patch actuators. Typical bimorph actuators have a displacement of less than 500 microns and force less than 2.5 N. These kinds of actuators take advantage of the strain in the direction that is perpendicular to the polarized direction of the piezoelectric materials. Unlike that, stack actuators take advantage of strain in the polarized direction directly which is the most efficient way of utilizing piezoelectricity. This kind of piezoelectric actuator could produce displacement proportional to the thickness, typically in the order of 100 microns. It is also as stiff as piezoelectric materials, which means it can generate large forces, though the displacement is limited because of the tiny strain of piezoelectric materials.

Piezoelectric material has also been used in hydraulic application, starting from micro pumps. Micro pumps are small pumps, a more up-to-date definition restricts this term to pumps with functional dimensions in the micrometre range [24]. In 1995, Gerlach and Wurmus presented a micro pump driven by piezoelectric material [25]. In this design a pump pressure of up to 7 kPa and upper frequency limit of 10 kHz is achieved. In 1999, Jung-Ho Park [26] introduced a piezoelectric micro pump that drove the bellow at its resonant frequency. Maximum flow rate of 80 mm^3/s, maximum pumping pressure of 0.32 Mpa and maximum power of 8.7 mW are obtained at the driving frequency of 2 kHz. Mauck and Lynch [27] developed the various versions of new actuation systems consisting of a piezoelectric-hydraulic pump driven by a high voltage piezo stack and hydraulic cylinders.

Konishi has developed the first macro-scale piezoelectric-hydraulic pump using a piezoelectric stack actuator [28]. It claims that the maximum pumping power for piezo actuators is 34 W with 300 Hz resonant frequency. However, this paper was published in 1993. The technology of piezoelectric material has advanced so much in the last two decades that the maximum pumping power for piezo actuators in the current market should be reassessed.

1.2.4. Power Transmission Device

Instead of using piezoelectric material as actuation, another mechanism is designed to be used as power transmission device to achieve a compact design of diaphragm pump. The use of power transmission device or system to connect pump liquid end with motor end is a relatively recent development. The first system of this sort was introduced to the market in 1960s and 1970s. Back then it was primarily utilized in a construction dewatering system so that the motor which it gets connected to could be located well away from construction site [17]. The current popular ones are sliding crank, cam shaft and gear transmissions.

The advantage of some power transmission device includes the ability to be located close to pump or in a more protected or accessible area. Also, with power transmission system, the flow rate of pump could be easily varied by regulating the

effective stroke length of the device towards the diaphragm. For example, effective stroke length of a sliding crank could be adjusted by changing the relative position between the rotating shaft and the plunger; effective stroke length of a gear transmission could be changed through changing gear ratios. Other advantages include the ease of automation for automatic or remote control, and safety because there is no high-voltage electricity in the fluid.

However, a major criticism of these mechanical power transmissions is its large volume and large number of components. The footprint of a pump with one of these mechanisms is very big, especially compared with centrifugal pumps of similar power. None of these mechanisms is suitable for a borehole application where space is highly restricted. The efficiency is also a big concern because there is power loss due to its friction.

The mechanism that is introduced in this thesis is inspired by algebraic screw. The algebraic screw pair or A-pair, is a novel kinematic pair based on a specific configuration of parallel manipulators called the Griffis-Duffy platform (GDP) [29]. The GDP is a special configuration of the six legged, six degree-of-freedom (DOF) Stewart-Gough platform (SGP) that converts rotary motion to linear motion, or vice versa [30]. The rationale behind proposing the algebraic screw pair is based on the hypothesis that it will converts rotary motion of a motor into linear motion, and thus form the suction and discharge stroke of a diaphragm pump.

One of the configurations of the mechanism is shown in Figure 1-4. It is originally designed to be used in vehicular suspension system [31]. Other than that, similar mechanisms have also been used in flight simulators and milling machines [32]. These mechanisms have not been used in hydraulic applications before.

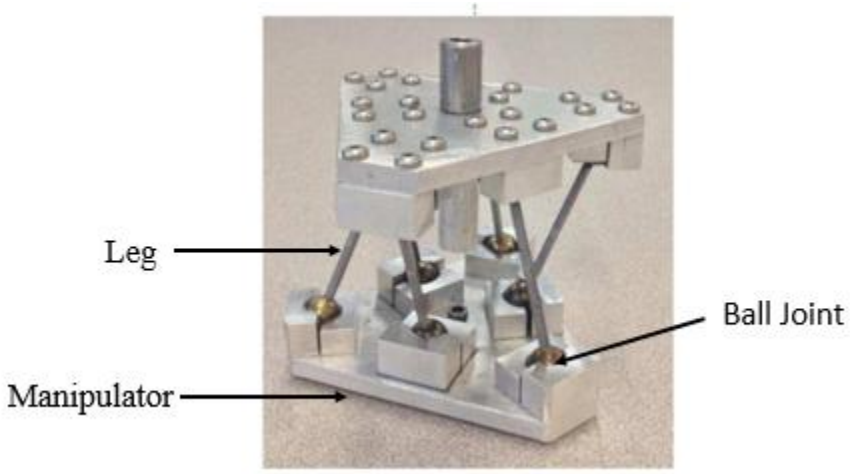

Figure 1-4. Algebraic Screw for Vehicular Suspension System

The way that it converts rotary motion to linear motion is illustrated in Figure 1-5. If the bottom manipulator rotates and the top manipulator remains still, the angle between the two manipulators changes. Also a distance change between the two manipulators is generated. As shown in Figure 1-5, the top manipulator in the left diagram is slightly lower than the one in the right diagram.

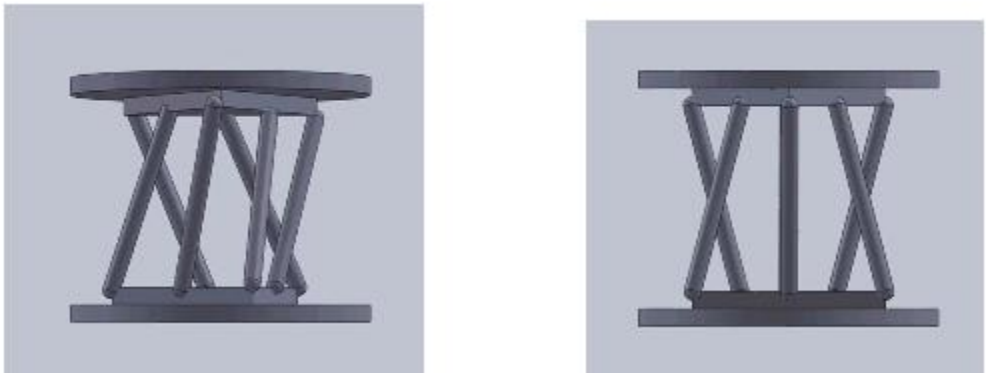

Figure 1-5. Snapshots of Algebraic Screw in Two Statuses

A formula describing the separation of two manipulators δ as a function of the rotation angle θ is obtained in [31].

$$\dot{\delta} = -\frac{a^2 \sin\theta}{6\sqrt{l^2 - \frac{a^2}{12}(5 - 4\cos\theta)}}\dot{\theta} \tag{1.1}$$

where a stands for the length of the triangle side and l stands for the length of the leg, as shown in Figure 1-6. This equation describes the relationship between the rotational and translation speeds of the two manipulators of the algebraic screw.

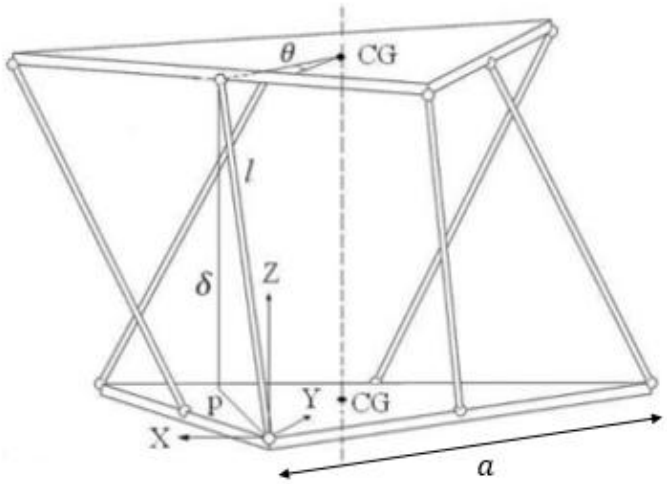

Figure 1-6. Algebraic Screw Schematic

At static equilibrium point, the separation distance between the two manipulators is δ_0 and the rotational angle is θ_0. An approximation of the relationship between the translation and rotation speeds about the static equilibrium operating point could be expressed as

$$\dot{\delta} = c\dot{\theta} \tag{1.2}$$

where c is given by

$$c = -\frac{a^2 \sin\theta_0}{6\delta_0} \tag{1.3}$$

The advantage of this mechanism is its high efficiency. In [31], it is claimed that the proposed algebraic screw has an estimated efficiency of 0.92, which is significantly higher than other mechanisms. Also the working frequency for this mechanism could be up to 5.6 Hz. But it also has its disadvantages. The rotary end could only rotate a maximum of 120º before the legs bump into each other. At the same time the linear motion end proceeds a distance of 3 cm assuming the diameter of the plates is 3.5".

This means that the rotary motor that actuates it needs to change direction every time after 120º of rotation and that a control system needs to be included to control and monitor the rotation which complicates the design.

Another mechanism that could be suitable for this project is cylindrical cam and followers. The cam is a machine element used to drive another element, called a follower, through a specified motion by direct contact [33]. Cam-and-follower mechanisms are simple and inexpensive, have few moving parts, and occupy very little space. Furthermore, follower motions having almost any desired characteristics are not difficult to design. For the above reasons, cam mechanisms are used extensively in modern machinery.

A cylindrical cam and follower mechanism could also be called a barrel cam and follower. It has many different forms. The more common one is with a rotating cam with a smooth curved profile and at the same time the follower is having a linear motion, with its speed relative to the shape of the curved profile. Different aspects of cylindrical cams have been focused on in research. The pitch curve of a cylindrical cam is a complex spatial curve, so that it is hard to design the pitch curve of it based on the motion law of the follower. Scholars all over the world have proposed many methods to calculate the planar expansion pitch curve coordinates as well as its radius of curvature on the cam. For example, Hidalgo-Martinez [34] discussed the application of Bezier curves for designing cams and a numerical method was proposed to optimize the design of the cam profile using a Bezier ordinate as an optimization parameter. This kind of cam follower mechanisms is suitable for applications where the space is restricted and very high forces are involved. Thinh and Joong [35] proposed a method of designing flexible cam profiles using smoothing spline curves. However, it is still necessary to find a method with the characteristics of uncomplicated, high precision and obvious geometric property, considering the practical engineering applications. Three-dimensional (3D) expansion method is an error-free method to expand the pitch curve of a cylindrical cam, which was proposed by Yong [36], Chen and Wu, and so on. However, they have not performed further research on the radius of curvature.

Cam and followers are widely used for packaging machines. It also plays an important role in printing presses, shoe machinery, textile machinery, gear-cutting machines and screw machines. The variety of different types of cam and follower systems that one can choose from is quite broad which depends on the shape of contacting surface of the cam and the profile of the follower. Compared with other mechanisms, cylindrical cam mechanisms have the advantages of small size, compact structure, good rigidity and high driving torque.

1.3. Outline

At the early stage of this project, various solutions are considered to improve pump designs for deep well borehole applications. The original idea is to use piezoelectric material for pump actuation because of its capability to generate high force and to work under extremely high frequency. After preliminary assessment, it turns out that piezoelectric material has its limit of power and it is not enough to actuate pumps in slurry applications. Then efforts are put into developing a new power transmission device which is efficient and has a simple and compact structure. Different mechanisms are developed and a prototype for pump is built using one of the new mechanism designs to prove functionality.

Following the introduction, Chapter 2 describes the different solutions proposed, including using piezoelectric material for actuation and using a new design of a power transmission device. Transmission Roller I is chosen as the final solution. Chapter 3 presents the building process of the pump prototype using the transmission roller. Chapter 4 builds mathematical models to calculate the transmission roller efficiency and loading force estimation. A finite element analysis of the stress distributed on the transmission roller is also carried out. Chapter 5 focuses on the pump test procedure and results. Chapter 6 presents analysis on different parameters for the prototype and the final production design based on the test results. Chapter 7 gives a conclusion of the work presented in this thesis as well as recommendations for future work.

Chapter 2.
Proposed Pump Design

A compact pump design for a deep well application is sought after for this project. This pump should be able to deal with slurries and other highly viscous or erosive liquid. It should also be of a relatively small volume which is suitable to be put through a borehole. At the same time, mechanical efficiency of the design should be comparable to or higher than pumps used in similar situations today.

Diaphragm pump is chosen as the basic pump model for this project due to the following reasons. Firstly, compared with centrifugal pumps, diaphragm pump could handle highly viscous fluid and slurries better. Flow rate and viscosity of the fluid do not have much impact on the output pressure of a diaphragm pump. Secondly, diaphragm pump is more suitable for a slurry application because of its flow rate pressure performance relationship. Diaphragm pump maintains a constant flow rate regardless of pressure, thereby tending to “purge” any plugging effect. Centrifugal pumps don’t have this feature because increased pressure to purge plugging effect is generated at the expense of reduced flow rate which might be inadequate to hold and keep slurries flowing in the pipe. Thirdly, most of the key pump components are protected from the transferred fluid by the diaphragm, so a diaphragm pump tends to have a longer lifetime. Also there is zero leakage because all the fluid is contained within the diaphragm and there is no need for seals and packing. This is often a preferred feature especially in the oil and gas industry.

Despite of all advantages and preferable features, the huge volume of the power transmission system is still a problem. Many options have been considered to achieve a compact design of a diaphragm pump. In this chapter, the possibility of utilizing piezoelectric material as actuation is first assessed. Though piezoelectric actuators are known for their ability to generate large force and work with high frequency, the

maximum working power and maximum pressure generated turn out to be both very little for a deep well pump. Another solution is proposed using a novel mechanism, named as transmission roller, to replace the original space-consuming power transmission system. Transmission roller converts rotary motion into linear motion and it is inspired by algebraic screw which is claimed to have high efficiency. Different versions of the transmission roller are also introduced in this chapter.

2.1. Piezoelectric Actuator

The first approach is to avoid the bulky power transmission system by using novel ways to actuate the pump. The three conventional ways for pump actuation are mechanical, hydraulic and pneumatic actuation. Other less common actuation methods use electric linear motors, electromagnetic motors, pneumatic motors or smart material actuators. Among smart materials, piezoelectric material is being applied more and more in hydraulic and other applications.

Figure 2-1 is a representation of a pump actuated by piezo material. The piezo actuator is acting directly on the diaphragm of the pump without any transmission mechanism in between. The thickness of the piezo actuator changes when an electrical voltage is applied, which incurs the suction and discharge stroke of the pump. The ideal situation is to put several piezo stack actuators around the diaphragm or even roll the stack piezo actuator around the diaphragm to generate as most power as possible for the pump. Compared with conventional diaphragm pumps, this would be a rather compact design where the power transmission system or device is eliminated.

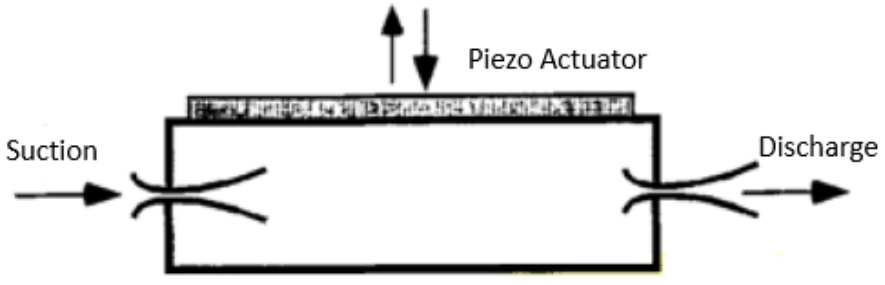

Figure 2-1. Piezo Actuated Pump Schematic

Piezoelectric motors are being considered here because of the large forces that they could generate and high frequency that they could operate at. Physik Instrumente (PI) is considered a global market and technology leader in the field of precision positioning technology with accuracies down to nanometers. It also develops and manufactures high-quality piezoceramic materials as well as actuator or sensor piezo components. The piezoelectric actuators provided by PI could reach up to 70 kN while the resonant frequency is 7 kHz, as shown in Appendix A. However, due to the small strain that a piezo actuator generates, the power generated from piezo is quite limited and is not sufficient to generate enough pressure for a deep well pump. Its feasibility regarding to power and the pressure requirement is assessed in this section.

Electroactive Polymers (EAP) has also been considered to actuate the pump. Electroactive polymers are polymers that exhibit a change in size or shape when stimulated by an electric field. Actuators and sensors are the most common applications of this type of material. Table 2-1 is the comparison for some basic parameters between EAP and Piezo. Through this comparison, it is shown clearly that piezoelectric material could generate more pressure which is more suitable for deep well applications. Thus piezoelectric material is the more suitable material for this project given the requirements.

Table 2-1. Physical property comparison between EAP and Piezoelectric

Actuator Type	Actuator Name	Maximum Strain (%)	Maximum Pressure (MPa)	Elastic Energy Density (J/cm3)
Electroactive Polymer	Acrylic	215	7.2	3.4
	Silicone (CR19-2186)	63	3	0.75
Piezoelectric	Ceramic (PZT)	0.2	110	0.1
	Single Crystal (PZN-PT)	1.7	131	1
	Polymer (PVDF)	0.1	4.8	0.0024

In this section, PI piezo actuators are taken to represent the current level of piezoelectric technology. They are being assessed in this section to see if they are feasible for deep well borehole applications in terms of power and pressure. Specifications for deep well applications from Toyo Pumps are used and compared with.

2.1.1. Feasibility in terms of Power

The approach taken to assess the feasibility of piezoelectric actuators in terms of power is by comparing the minimum power needed to generate the required head for the pump with the maximum power that a piezoelectric actuator could generate. According to this comparison, the number of actuators needed could be estimated.

According to the specifications stated in Chapter 1.1 from Toyo Pumps, the pump requirements could be listed as following. To differentiate these parameters of values provided by Toyo Pump from the actual pump prototype parameters measured or calculated later in this thesis, a semicolon ' is added for some of parameters in this section, which means that they are only used for piezoelectric actuator assessment. The required pump output pressure $p_{out}{}' = 1000\ psi$, the required pump input pressure $p_{in}{}' = 14.7\ psi\ (1\ atm)$, the minimum pump capacity $Q' = 50\ GPM$, the maximum pump diameter $d' = 3.5\ in$, the body length of the pump $Z' = 35\ in$.

The minimum pump head required h' is calculated as below [12]:

$$h' = \left(\frac{p}{\rho g} + \frac{v^2}{2g} + z\right)_{out} - \left(\frac{p}{\rho g} + \frac{v^2}{2g} + z\right)_{in} \approx \frac{p_{out}{}' - p_{in}{}'}{\rho g} + \frac{\left[\frac{Q'}{\pi\left(\frac{d'}{2}\right)^2}\right]^2}{2g} + Z' \tag{2.1}$$

Water is assumed the transferred fluid for this assessment, so $\rho = 1 \times 10^3 kg/m^3$. The minimum power required from the actuator is obtained assuming the pump efficiency is 100% and it is calculated as below [12].

$$P_{min}{}' = \rho g Q' h' = Q'\left(p'_{out} - p'_{in} + \frac{8\rho {Q'}^2}{\pi^2 {d'}^4} + \rho g Z'\right) \approx 21.461\ kW \tag{2.2}$$

Now the maximum power that a PI actuator can provide is calculated to be compared with the minimum power required by the pump. All the equations used for PI actuators are provided by PI website [37]. PI actuator P-056 .90P is chosen here as it is one of the PI actuators generating the highest force. It is also proven to be able to generate the most power using the method introduced below.

There are several basic parameters of a piezoelectric actuator. *Blocking force* F_{max} is the maximum force generated by the actuator. This force is achieved when the displacement is completely blocked, i.e. it works against a load with infinite stiffness. *Nominal displacement* ΔL_0 is the displacement achieved by the actuator when no force is generated or no load is applied. Stiffness is the rigidity of an object and it is usually defined as the ratio of force that applied on the body and the displacement produced by the force [38]. A piezoelectric actuator also has a definite stiffness and it is the key parameter which decides its performance [39]. *Stiffness* of a piezoelectric actuator k_A equals to the ratio of blocking force F_{max} and nominal displacement ΔL_0. All of the above parameters could be found in the technical specification table of a piezoelectric actuator.

In order to calculate the maximum power of an actuator, a simple virtual system is built consisting of a piezoelectric motor and a spring as load, shown in Figure 2-2. It is assumed that when actuator is inactive, the spring is at its natural length. When electric voltage is applied to the actuator, it starts to generate force and displacement. A spring is compressed until the force generated by the actuator is equal to the force generated by the compressed spring. A spring is used because it is easy to express the work done by the actuator in terms of the potential energy of the spring.

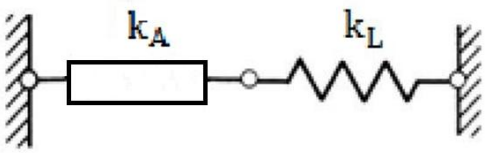

Figure 2-2. Actuator and Load Spring Model

Given the stiffness of the load k_L, the final displacement ΔL of the actuator could be obtained [37].

$$\Delta L = \Delta L_0 \times \frac{k_A}{k_A + k_L} \tag{2.3}$$

Resonant frequency without load f_0 is the limit of the frequency that the actuator could work with when there is no load. However, when there is a load, the resonant

frequency would decrease and the decreased resonant frequency $f_0{}'$ could be expressed as below [40].

$$f_0{}' = \frac{1}{2\pi}\sqrt{\frac{k_A}{m_{eff}}} \tag{2.4}$$

where m_{eff} is the effective mass of the actuator. In this case, the effective mass could be expressed as below.

$$m_{eff} = \frac{k_L \Delta L}{2g} \tag{2.5}$$

In the system shown in Figure 2-2, the piezoelectric actuator could generate a reciprocating motion if the direction of the electric voltage is alternating. The maximum displacement generated is ΔL and the maximum frequency that it could work with is $f_0{}'$. Thus the maximum power that this actuator could generate in an ideal situation P_A is obtained using Eq. 2.3 to Eq. 2.5.

$$P_A = \frac{1}{2}k_L \Delta L^2 f_0{}' = \frac{1}{4\pi}\sqrt{\frac{2g\Delta L_0{}^3 k_A{}^4 k_L}{(k_A+k_L)^3}} \tag{2.6}$$

The specifications for PI actuator P-056 .90P are displayed in Appendix A. The nominal displacement $\Delta L_0 = 180\,\mu m$. Stiffness $k_A = 390\,N/\mu m$. Using Matlab optimization toolbox, the maximum value for P_A could be obtained when $k_L = 195\,N/\mu m$. The other parameters are obtained as well.

$$P_A = 127.7W \tag{2.7}$$

$$\Delta L = 120\,\mu m \tag{2.8}$$

$$f_0{}' = 90.97\,Hz \tag{2.9}$$

This means that the maximum power that PI actuator P-056 .90P could achieve in this system is 127.7 W. Compared with the minimum power that is needed to actuate the pump $P_{min}{}' = 21.461\,kW$, the power generated by PI actuator is 168 times smaller. In other words, 168 piezoelectric actuators are needed at least to achieve the minimum

power needed for pump actuation. It is obviously not feasible to use piezoelectric actuators for this project in terms of power generation and requirement. However, improvement for piezoelectric technologies is still seen in the last two decades since the maximum power generated by piezoelectric actuators reported by K. Konishi in [28] was only 35 W.

2.1.2. Feasibility in terms of Pressure

Another approach to assess the feasibility of piezoelectric actuators is by comparing their ability of pressure generation with the required pressure output of the pump. Using the specifications from Toyo Pumps, the pressure output requirement is $p'_{out} = 1000\ psi = 6894.8\ kPa$.

The maximum pressure generated by a piezoelectric actuator for the pump could be estimated as the ratio of blocking force F_{max} and peripheral area of the diaphragm. Given the structure of a diaphragm pump, the peripheral area of the diaphragm is always smaller than the peripheral area of the pump body. P-056.90P actuator is again used for this assessment because it is able to generate the biggest blocking force among PI actuator product. Thus the maximum pressure that P-056.90P could generate in this diaphragm pump p_a is obtained.

$$p_a = \frac{F_{max}}{\pi d' Z'} = 885.7\ kPa \tag{2.10}$$

Compared with the required pressure 6895.8 kPa, the maximum pressure generated by one P-056.90P actuator is almost 8 times smaller. In other words, at least 8 P-056.90P actuators are needed to generate the required pressure in this diaphragm pump. It is also not feasible to use piezoelectric actuator in terms of pump pressure requirement and generation.

Based on the above assessments, piezoelectric actuator is not a feasible solution for this project, due to its limited power and pressure generation compared with pump requirements for the deep well applications.

2.2. Transmission Roller

Another approach to achieve a compact design for diaphragm pumps is introduced in this section. Instead of using a traditional large power transmission system for diaphragm pumps, such as sliding crank, a novel mechanism is designed and named as transmission roller based on its function.

This design is inspired by the structure and function of algebraic screw. As introduced in Chapter 1.2.4, the algebraic screw pair or A-pair, is a novel kinematic pair based on a specific configuration of parallel manipulators called the Griffis-Duffy platform (GDP) [29]. The GDP is a special configuration of the six legged, six degree-of-freedom (DOF) Stewart-Gough platform (SGP) that converts rotary motion to linear motion, or vice versa [30]. Algebraic screw is also claimed to have an estimated efficiency of 0.92 [31].

Considering the simplicity of its structure, and its core function of converting rotary motion into linear motion, and its claim of high efficiency, algebraic screw is very suitable to be applied in the pump design. Algebraic screw could be applied to convert the rotary motion of a motor into the linear motion of its manipulator, thus forming the suction and discharge stroke of a diaphragm pump. However, in order to have a reciprocating translation motion of the upper manipulator, the rotation motion of the lower manipulator needs to change direction every 105º before the legs collide with each other. This means that the motor needs to change direction after 105º of rotation and position feedback control might be needed for the system. This is a disadvantage of the algebraic screw because it complicates the system.

Transmission roller is a design inspired by algebraic screw. It inherits the core motion transmission function from algebraic screw. It also has the preferable feature of compactness, which has a regular outer shape and could fit into a tubular structure very well. It is also promising to have a high efficiency just like algebraic screw. Even better than algebraic screw, a direction change of rotation motion is not needed to generate a reciprocating translation motion. The manipulator below only needs to rotate constantly in one direction.

2.2.1. Transmission Roller I

The first design of transmission roller is shown in Figure 2-3. Transmission roller I consists of two primary parts: rotary revolver and linear plunger, as shown in Figure 2-4. Rotary revolver is in the shape of a hollow cylinder. It has a shaft in the end which is to be coupled with a rotary motor. The revolver has four bearings attached onto its inside wall after assembly. When the revolver is actuated by a motor, the four bearings will rotate with the revolver together. The linear plunger has two tracks on its outer wall in the shape of sine curves. The rotation of the plunger is prohibited by the two pins inserted into the corresponding holes on the plunger through the slots on the pump tube. The pins guarantee the alignment of the holes on the plunger and the slots on the pump tube. As a result, the plunger could only moves in the vertical direction with a reciprocating manner. In this way, the rotation of the revolver is converted to the linear motion of the plunger. Unlike algebraic screw, the reciprocating motion of the plunger could be achieved without rotation direction change of the revolver.

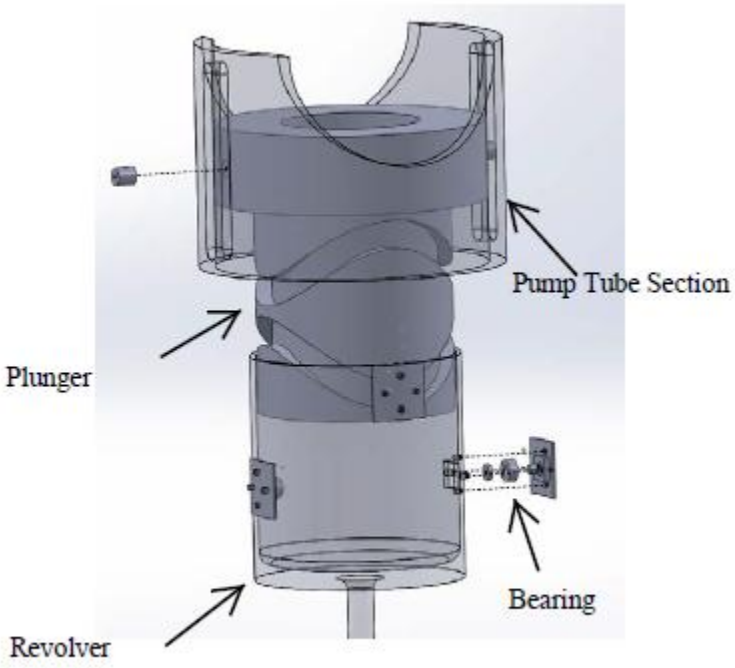

Figure 2-3. Transmission Roller I Overview

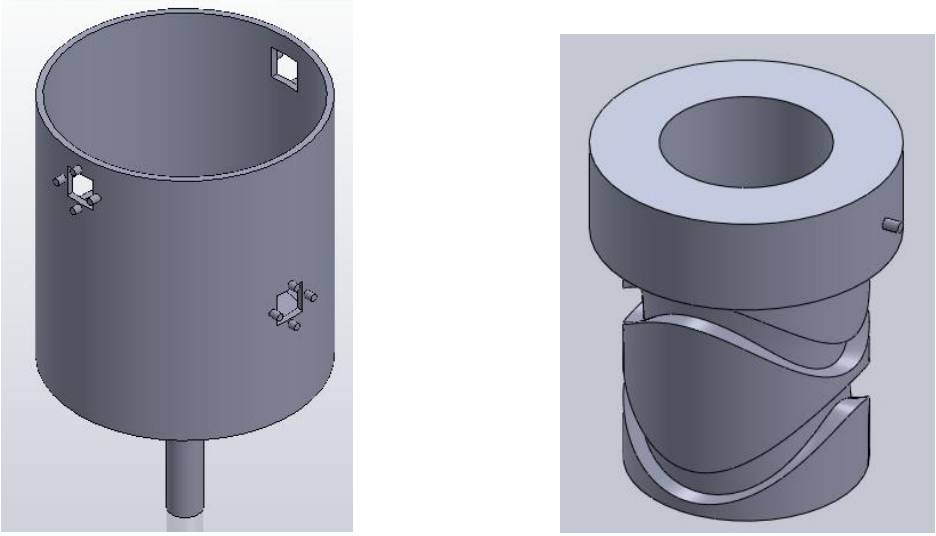

(a) Revolver (b) Plunger

Figure 2-4. Primary Parts of Transmission Roller I before Assembly

Figure 2-5 presents the shapes of the tracks unwrapped onto a planar surface together with the locations of bearings. The four bearings on the revolver can be divided into two groups according to their different heights of locations. Bearings 1 and 2 roll on the upper track while bearings 3 and 4 roll in the lower track. There is a 90º phase shift between two tracks. Thus, when assembling the linear plunger with rotary revolver, the four bearings could all fit in and roll on the tracks at the same time.

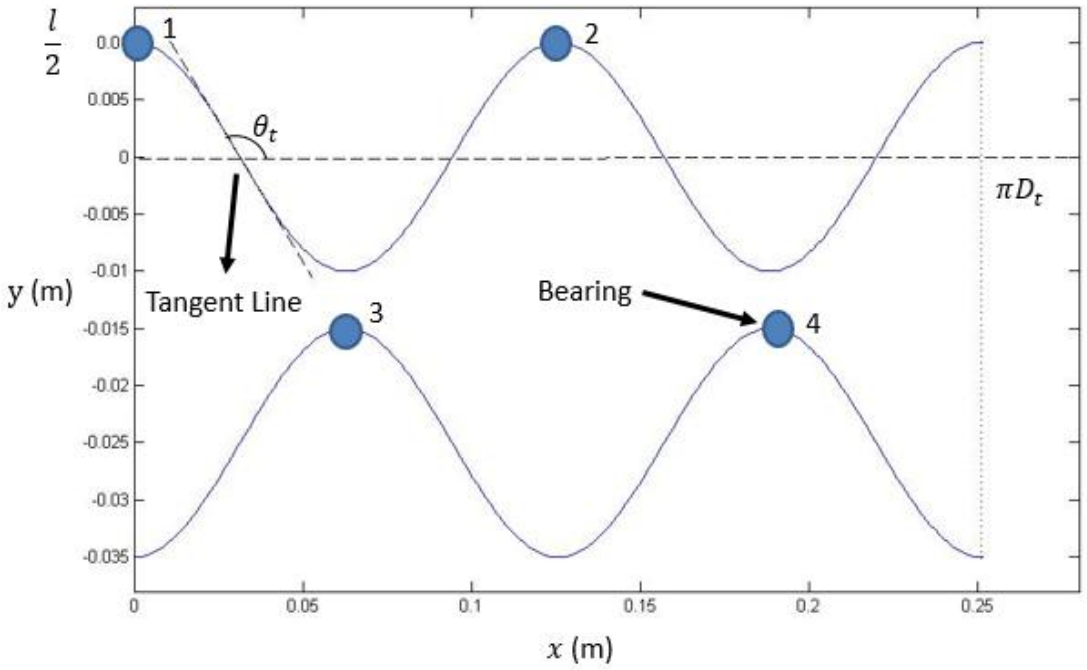

Figure 2-5. Transmission Roller I Tracks Unwrapped onto a Planar Surface

Now the relationship between the rotary motion of the revolver and the linear motion of the plunger is analyzed here. The connection between the revolver and the plunger is the four bearings whose motions are analyzed first. Since all the bearings go through similar motions, only bearing 1 is analyzed and its motion function is obtained. (x, y) are the coordinates indicating the location of bearing 1 on the unwrapped surface shown in Figure 2-5. Both x and y are functions of time t. Assume $t = 0$ in Figure 2-5. Since the tracks are in the shape of a sine curve, the relationship between x and y is given by

$$y = \frac{l}{2}\sin\left(\frac{4}{D_t}x + \frac{\pi}{2}\right) \tag{2.11}$$

where l is the amplitude of the track curve and D_t is the diameter of the plunger for the track part. The cycle length of the sine curve is equal to $\frac{\pi D_t}{2}$ in this case.

Assuming constant rotation speed for the revolver, x could be expressed in terms of t as below.

$$x = \omega t \times \frac{D_t}{2} = \frac{1}{2}\omega t D_t \tag{2.12}$$

where ω is the rotary speed of the revolver. It is also the rotary speed of the motor.

When bearing 1 is located at the top of the track, the plunger is going through its lowest location. Assuming the displacement of the plunger is 0 at the midpoint of its full stroke, the function for its displacement z is given by

$$z = -y = \frac{l}{2} sin\left(2\omega t - \frac{\pi}{2}\right) \tag{2.13}$$

Eq. 2.13 describes the relationship between the plunger displacement z and the revolver rotary speed ω.

If this mechanism is applied to a diaphragm pump, some parameters of this mechanism will influence its performance. Flow rate of the pump is directly related to the amplitude of the track l, which is actually equal to the stroke length. At a certain motor speed ω, a larger flow rate could be achieved with a larger stroke length. However, given a certain plunger diameter D_t, the stroke length or the amplitude l cannot be set too large. This is because with a larger amplitude l, the track becomes steeper which could be indicated by the gradient of the tangent line shown in Figure 2-5. The gradient of the tangent line when $x = \frac{\pi D_t}{8}$, where the track is steepest, could be expressed as

$$\dot{y}_{x=\frac{\pi D_t}{8}} = -\frac{2l}{\mathrm{D_t}} \tag{2.14}$$

With steeper tracks, the revolver will experience a harder time actuating the plunger in the vertical direction and the mechanism is more likely to fail. Thus the amplitude l should be set appropriately. For the prototype of transmission roller I, the amplitude is set as 0.8”, while the sine curve gradient at the origin is 0.6.

In addition, the cycle length of the sine curve is also related to the pumping speed. At a certain motor speed ω, a shorter cycle length indicates a faster pumping speed. In this design, there are two complete cycles of sine curve around the plunger. In

other words, when the rotary motor shaft has completed one cycle, the pump has completed two pumping cycles, including two discharge strokes and two suction strokes. The relationship between pump speed n and motor speed ω is given by

$$\omega = \frac{2\pi n}{2} = \pi n \tag{2.15}$$

Transmission roller I is a compact design which converts rotation motion to linear motion without the need for direction change. It could replace the conventional power transmission device for diaphragm pumps. However, the stroke length of the pump would be limited because of the constraint on the amplitude of the tracks. This means the volume of the fluid transferred per pump cycle is limited. An extended version of transmission roller is introduced in the next section offering a solution which could overcome the disadvantage of limited stroke length.

2.2.2. Transmission Roller II

An extended design for transmission roller is presented in this section. It aims to overcome the constraint of limited stroke length. This design offers a way to modify transmission roller to achieve any stroke length that is desired without making the tracks steeper. And it still guarantees the diameter of the plunger within a certain diameter, which is 3.5” in this case.

An example of the modified version is shown in Figure 2-6. This design also consists of two primary parts: a rotary revolver and a linear plunger, as shown in Figure 2-7. The way it works is similar to Transmission Roller I. The rotary revolver has two bearing groups attached onto its inside wall after assembly. Each bearing group has three bearings connected together, as shown in Figure 2-8. When actuated by a rotary motor, the bearing groups will rotate with the revolver together. Compared with the revolver for Transmission Roller I, the revolver in this version has more cut on the cylindrical wall. With these cuts, it is more convenient for bearing groups assembly and easier to see how the bearing groups work when prototyping. The plunger also has tracks on its outer wall in the shape of sine curves. It is also locked from rotation and only moves in a reciprocating manner in the vertical direction. The bearing groups roll

along the tracks, generating the translation motion of the plunger. In this way, the rotation of the revolver is converted to the linear motion of the plunger.

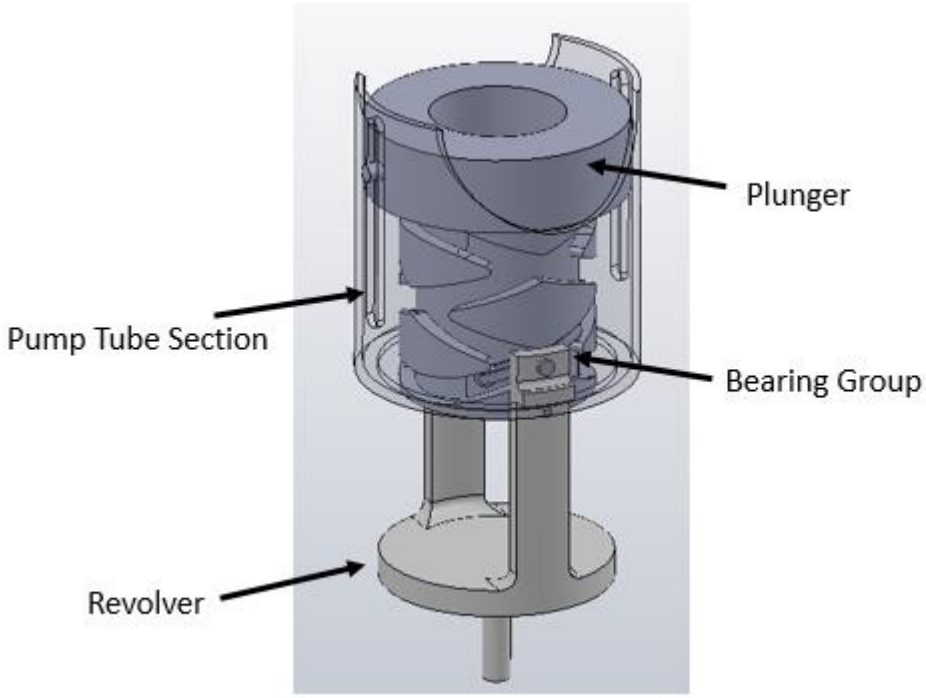

Figure 2-6. Transmission Roller II Overview

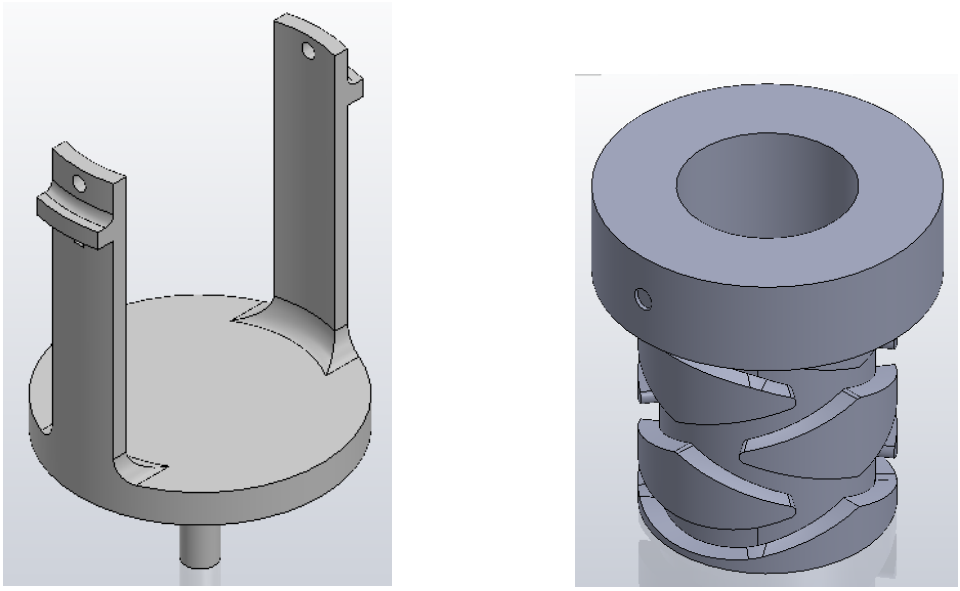

(a) Rotary Revolver (b) Plunger

Figure 2-7. Primary Parts of Transmission Roller II before Assembly

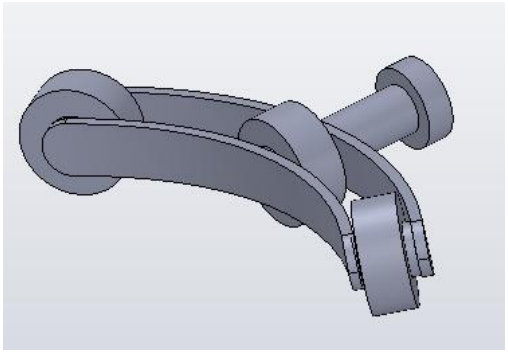

Figure 2-8. Bearing Group with Three Bearings

Figure 2-9 presents the shapes of the tracks unwrapped onto a planar surface together with the locations of bearing groups. The plunger diameter D_t for transmission roller II is kept the same as roller I for easy comparison. The track for bearing group 1 is drawn with a solid line while the track for bearing group 2 is drawn with a dotted line. It is obvious that the cycle length for each track is $2\pi D_t$, which is two times of the circumference of the plunger cross section circle. In other words, the bearing groups need to go around the plunger two times to finish one cycle of the track. There is a 180º

phase shift between two tracks so that the 2 bearing groups could fit in their separate tracks at the same time.

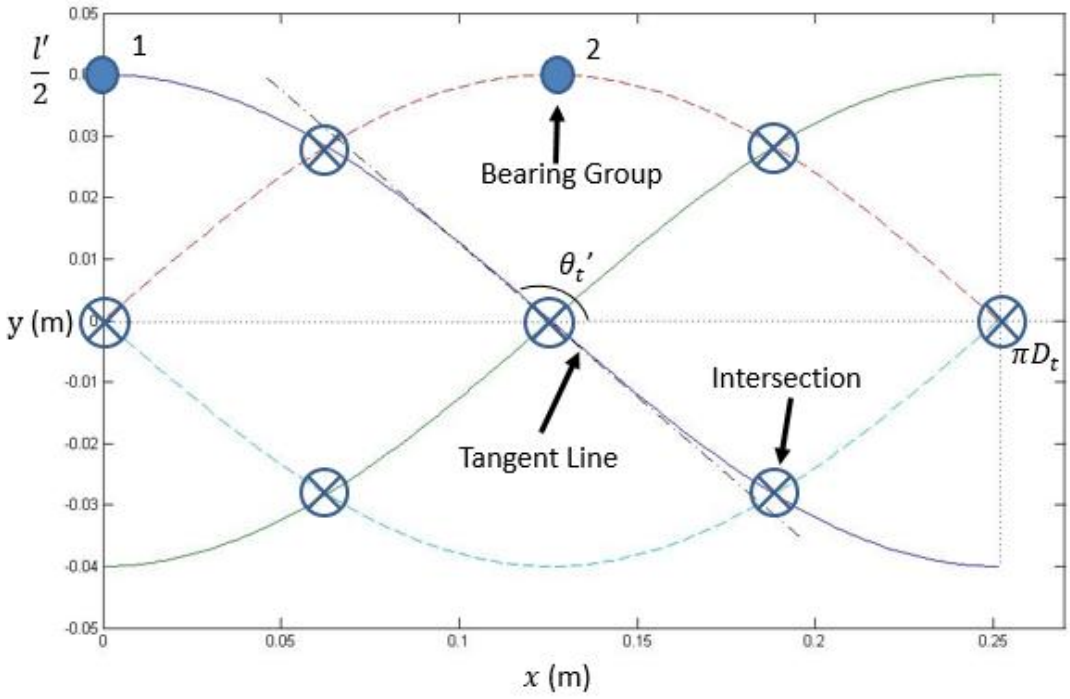

Figure 2-9. Transmission Roller II Tracks Unwrapped onto a Planar Surface

Similar to Transmission Roller I, the relationship between the rotary motion of the revolver and the linear motion of the plunger for Transmission Roller II could also be deduced using the same method. (x, y) are the coordinates indicating the location of bearing group 1 on the unwrapped surface. Both x and y are functions of time t, assuming $t = 0$ in Figure 2-9. When the bearing group is rolling around the plunger for the i^{th} time, the relationship between x and y is

$$y = \frac{l'}{2}\sin\left[\frac{1}{D_t}x + (-1)^{\mathrm{i}-1}\frac{\pi}{2}\right] \tag{2.16}$$

where l' is the amplitude of the tracks for Transmission Roller II. Same as Eq. 2.12, x could be expressed in terms of t as below.

$$x = \omega t \times \frac{D_t}{2} = \frac{1}{2}\omega D_t t \tag{2.17}$$

where ω is the rotary speed of the revolver. It is also the rotary speed of the motor. Assuming the displacement of the plunger is 0 at the midpoint of its full stroke, the function for its displacement z is given by

$$z = -\mathrm{y} = -\frac{l'}{2}\sin\left[\frac{1}{D_t}x + (-1)^{\mathrm{i}-1}\frac{\pi}{2}\right] \tag{2.18}$$

Compared with Transmission Roller I, roller II generates a bigger displacement with the same plunger diameter and similar steepness of the tracks. If applied to diaphragm pumps, it means bigger stroke length and bigger volume of fluid transferred per pump cycle. The gradient of the tangent line when $x = \frac{\pi D_t}{2}$, where the track is steepest, could be expressed as

$$\dot{y}_{x=\frac{\pi D_t}{2}} = -\frac{l'}{2\mathrm{D_t}} \tag{2.19}$$

where i is assumed to be 1. If the tracks for roller II and roller I have equivalent steepness, then $-\frac{l'}{2\mathrm{D_t}} = -\frac{2l}{\mathrm{D_t}}$ using Eq. 2.14 and 2.19. It could be deduced

$$l' = 4l \tag{2.20}$$

Eq. 2.20 indicates that Transmission Roller II increases the stroke length by 4 times than roller I of the same plunger diameter and equivalent track steepness. For Transmission Roller II, there is a half cycle of sine curve around the plunger. In other words, the bearing group needs to travel around the plunger two times to finish one track cycle. The relationship between pump speed n and motor speed ω is given by

$$\omega = 4\pi n \tag{2.21}$$

However, a big difference from Transmission Roller I is that the tracks in Transmission Roller II have intersections. There are 6 intersections in total shown as circled crosses in Figure 2-9, for the two intersections at two far ends are actually one. The design of bearing groups is aimed to keep rolling along the sine curve instead of going sideways at intersections. Three bearings are connected together forming a long

bearing group, as shown in Figure 2-10. Each bearing goes through the intersection one by one while the other two bearings which are still in the track controlling the rolling direction. However, the structure of this bearing group is somewhat complex and might be a weak point in the mechanism because of the small thickness of the racks that connect the bearings.

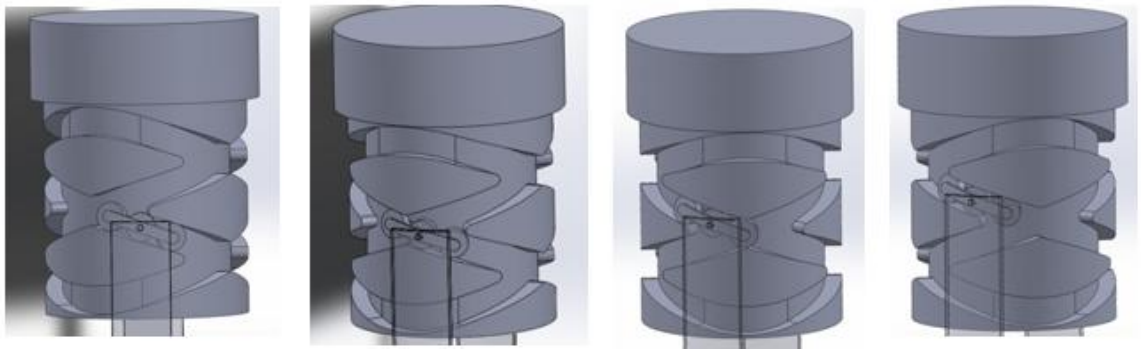

(1) (2) (3) (4)

Figure 2-10. Bearings Row

Transmission Roller II is an extended design based on Transmission Roller I. By using it as power transmission device for diaphragm pumps, a larger stroke length is achieved with the same plunger diameter and equivalent steepness of the tracks as Transmission Roller I. What has been introduced in this section is only one example of Roller II, with stroke length 4 times bigger than Transmission Roller I. The cycle length of the sine curved tracks is 2 times of the plunger circumference. Bigger stroke length could be achieved if the ratio between the cycle length of the sine curved tracks and the plunger circumference is changed from 2 to 3, 4, … ,n. One notable disadvantage of Transmission Roller II is the complex structure of the bearing group which compromises its reliability.

2.3. Conclusion

A diaphragm pump, utilizing Transmission Roller I as its power transmission device, is chosen as the final solution for this project. The structure of a diaphragm pump provides the ability to deal with slurries and other highly viscous or erosive liquid. Transmission Roller I is a compact and space-saving design in dimensions which could

fit well in a borehole of 3.5” diameter. Inspired by algebraic screw, transmission roller might inherit from algebraic screw the feature of high transmission efficiency, but it needs to be confirmed. Unlike algebraic screw, it requires no direction change of the motor. Transmission Roller II overcomes the constraint for stroke length. It could also be used as power transmission device for diaphragm pumps after confirming the structure integrity of its bearing group, especially for high output pressure applications. The chosen Transmission Roller I will just be referred as transmission roller in the rest of the thesis for the ease of description.

There are several major differences between the Transmission Roller and a cylindrical cam. Firstly, the tracks or profiles lie on the rotary party for the cylindrical cam while they lie on the linear part for the Transmission Roller. The Transmission Roller is designed this way so that the rotary part could be totally symmetric in its structure and thus has a more balanced performance. The other difference is that the Transmission Roller is perfectly lined up and compact in its structure with multiple supporting bearings, while the cylindrical cam usually has the follower on one side and only one supporting point. The Transmission Roller is more likely to withstand larger pressure and lead to a compact design which could fit in the borehole applications.

In order to perform further analysis of the transmission roller, a prototype of the diaphragm pump utilizing transmission roller is built and tested. Modifications are made both on the structure of the diaphragm pump and the transmission roller for simplicity of the prototype and for assembly.

Chapter 3.
Pump Prototype Fabrication

This chapter introduces the fabrication of the pump prototype using transmission roller as its power transmission device. The main purpose of building the prototype is to test the concept of transmission roller and learn from it. The prototype is also to be used for testing so that experimental data could be collected to analyze the efficiency of transmission roller.

The prototype design mainly consists of the following parts: motor, transmission roller, turntable, pump tube and valves. A CAD model of the prototype design is shown in Figure 3-1. Transmission roller converts the rotary motion of the motor into linear motion. This linear motion is utilized to pressurize or depressurize the fluid in the pump chamber and thus generates discharge and suction strokes. The way it works is similar to a diaphragm pump, however diaphragm is not present in this design.

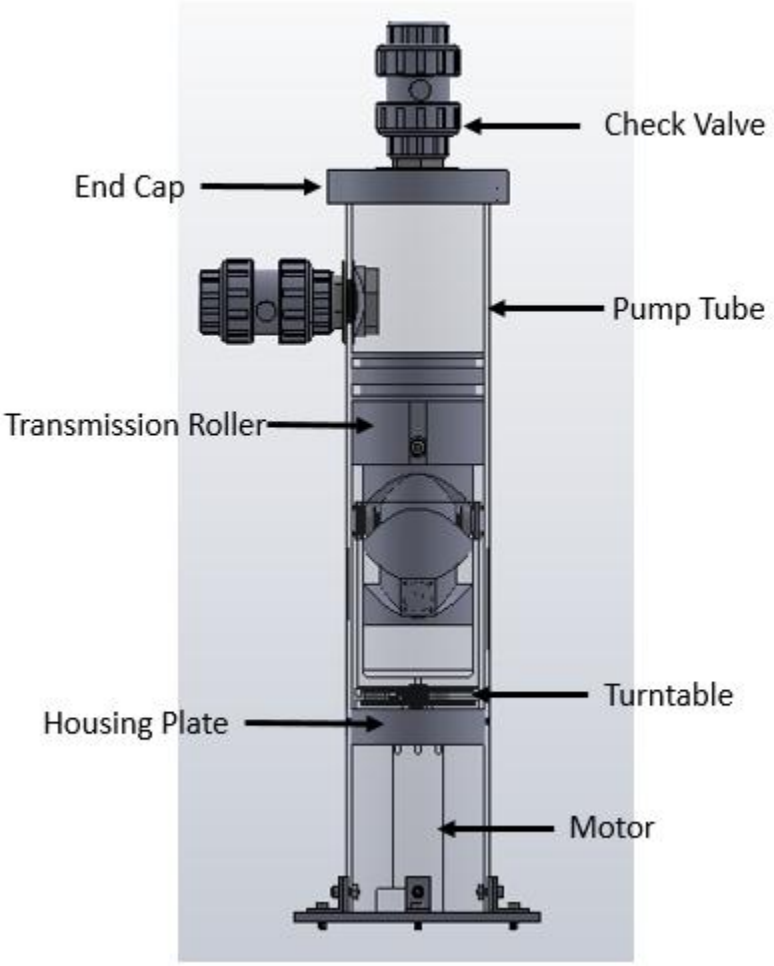

Figure 3-1. CAD Model of the Pump Prototype

Note that this prototype design is not a production design. A production design will be different in terms of material choice and the details of pump structure. One big difference is the existence of diaphragm in this case. Compared with traditional diaphragm pump as shown in Figure 3-1, the diaphragm separating the process fluid from hydraulic oil is absent in the prototype. This modification is made in order to simplify the fabrication process. Without the diaphragm, there is no need to have a separated oil reservoir. The structure of the prototype design is much simplified and the cost of fabrication is brought down significantly, while the functionally of transmission roller could still be validated. Of course, the diaphragm is irreplaceable and indispensable in the final production design because it plays an important role for separating the process fluid from other pump components.

3.1. Prototype Parts

3.1.1. Transmission Roller

Compared with the conceptual design of transmission roller proposed in Chap. 2.2, the model introduced in this section is with more structural details and ready for fabrication, as shown in Figure 3-2. The same as the conceptual design, transmission roller mainly consists of two parts, revolver and plunger. They are 3D printed because of their irregular shapes. It will be very expensive and impractical to machine those sine tracks. In this case, the 3D printer used is uPrint SE from Stratasys. Parts are printed with ABS material in ivory color and with a resolution of 0.01".The track width is 0.85".

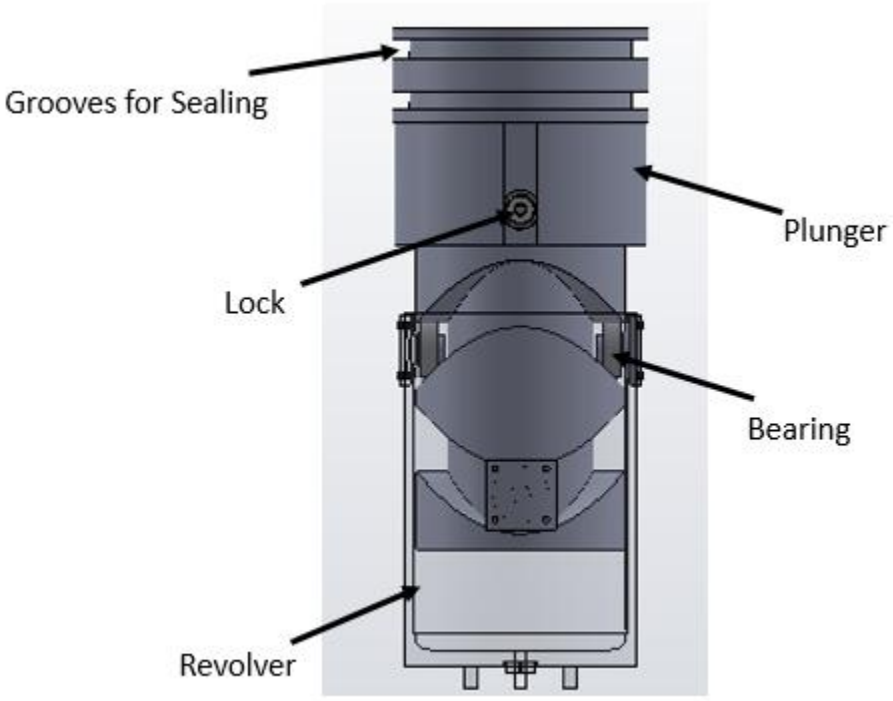

Figure 3-2. Prototype Transmission Roller

The revolver and the plunger are connected through steel ball bearings, with McMaster-Carr No. 6383K12. These bearings are plain open for 1/4" shaft diameter, 11/16" OD and 1/4" wide as shown in Figure 3-3 [41]. Steel bearings are chosen here because the connection point is where the loading force concentrates and thus needs to be as solid as possible. The amplitude of the force expected at the connection is high

relevant to the output pressure, the weight of process fluid and the plunger. Pulsations generated because of the discontinuous flow [42] also influence the connection. The surfaces which bearings are rolling on are finished by sand paper to reduce friction and thus increase efficiency.

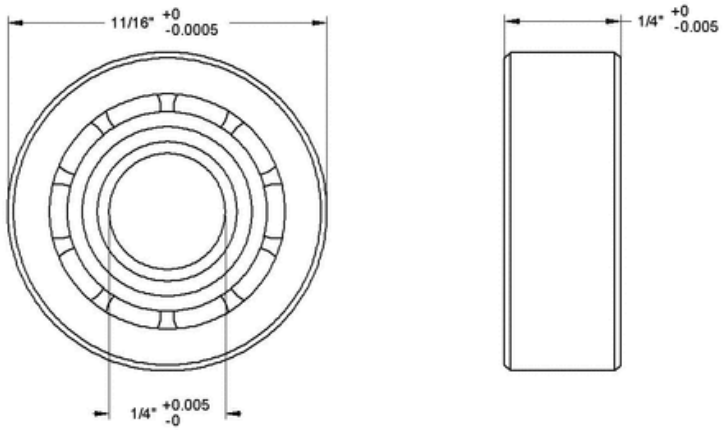

Figure 3-3. Steel Ball Bearing Dimensions

The plunger moves only in the vertical direction because of the side locks. Figure 3-4 shows the structure of one side lock with the other one hidden on the back side of the plunger. A shoulder screw is inserted into the side slot of the plunger with one end and the other end is secured onto the pump tube with a nut. This structure prevents the plunger from rotating. A ball bearing is put on the shoulder of the screw to reduce the generated friction when the plunger moves in the vertical direction.

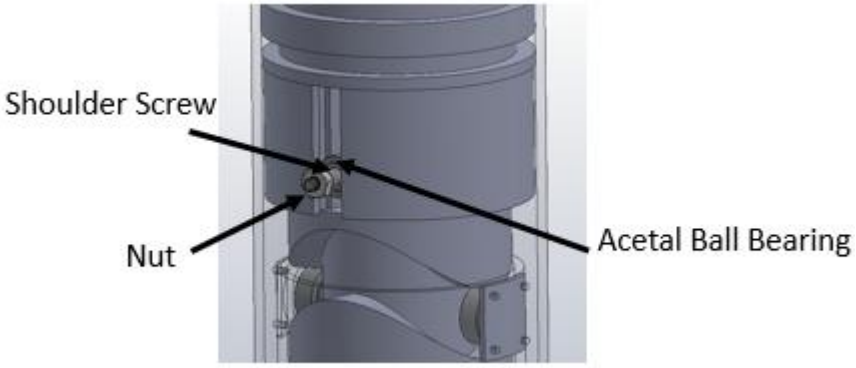

Figure 3-4. Structure of the Side Lock

Two acetal plastic ball bearings are chosen because this connection point is not expected to withstand big force. The Mcmaster-Carr No. for these bearings are 6455K7 [43]. They are lubrication free, 3/16” shaft diameter, 1/2” OD, 5/32” wide with glass balls inside, as shown in Figure 3-5.

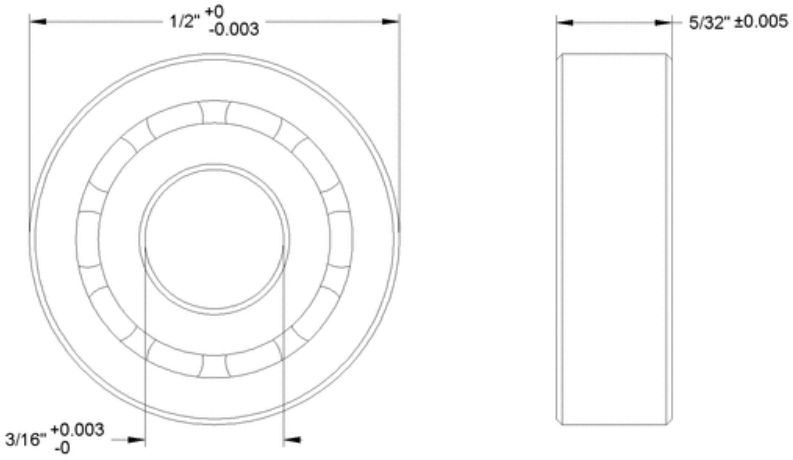

Figure 3-5. Acetal Ball Bearing Dimensions

U-cups are used for sealing and their grooves are located close to the top of the plunger. U-cups are a lip seal, named for the cross-section’s distinctive “U” shape. They are used for both dynamic and static applications. The “U” shape energizes the sealing lips as the application pressure increases. 8400 Nitrile NBR80A U-cups are used, with Sealsonline No. 840802750 [44], as shown in Figure 3-6. The groove diameter is set as 2.741” and the groove width is set as 0.291”.

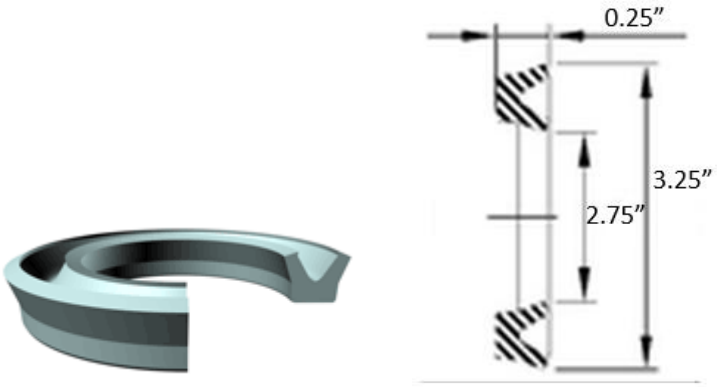

Figure 3-6. U-cups and Dimensions

As illustrated in Chap. 2.2.1, the shape of the transmission roller is important in deciding pump parameters such as flow rate and pump speed. In this prototype, the amplitude of the tracks l is 0.8" and the diameter of the plunger D is 3.25". The diameter of the plunger for the track part D_t is 2.65", and the cycle length of the sine curve $\frac{\pi D_t}{2}$ is 4.16". Assuming the pump speed n is 1 cycle/s, the ideal pump flow rate Q_i is give by

$$Q_i = \pi(\frac{D}{2})^2 ln = 1.72\ GPM \tag{3.1}$$

Note this prototype is built to validate the functionality of the transmission roller and it is not a production design. Compared with typical industrial requirements from Toyo Pumps, the generated flow rate by this prototype is quite small. Transmission Roller II should be used if bigger flow rate or stroke length is desired.

3.1.2. Motor, Housing and Shaft

The revolver is actuated by a rotary motor through a coupling shaft. The shaft goes through a housing plate, as shown in Figure 3-1. The housing plate, as shown in Figure 3-7, secures the motor to the pump tube and distributes all the forces including the weight of transmission roller and process fluid onto the pump tube instead of the motor.

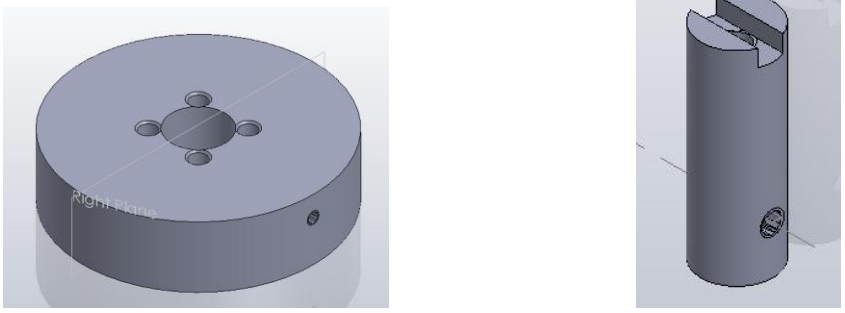

(a) Housing Plate (b) Coupling Shaft

Figure 3-7. Housing Plate and Coupling Shaft

Different motors have been used throughout the testing process. When demonstrating the movement of the transmission roller without water, a maxon A-max DC motor with a gearhead is used. The part No. is 236668 [45]. This motor is of 32 mm diameter and 20 Watt, with graphite brushes and terminals. The gearhead that is attached onto it is planetary gearhead GP 32 C. The part No. is 166931, [46]. Its gear reduction is 4.8 : 1.

However, when tested the pump with water, it turns out that maxon A-max motor is not able to generate enough power to actuate the prototype. This is because U-cup seals actually are generating more friction than expected when the plunger is reciprocating in the vertical direction. A more powerful DC motor is used to replace Maxon A-max 32 to compensate for all the frictions generated between the seals and the tube. The dimensions of the shaft and the housing plate changes accordingly to accommodate the new motor.

3.1.3. Turntable

When the pump works, the revolver is actuated by the motor while the housing plate is stationary and secured with the pump tube. Considerable frictions will be generated if the revolver and the housing plate are in direct contact. A turntable is added to the design between the revolver and the housing plate to reduce friction loss.The turntable used has a McMaster-Carr No. 1413T11 [47]. This is a light duty plastic turntable, of 3” diameter and 9/16” height. It is chosen because it is economic and practical for a prototype fabrication and because a metal version is much more expensive and not available in similar sizes.

Turntable consists of two clear plastic layers with three steel ball bearings between them. The top layer rotates simultaneously with the revolver while the bottom layer stays still with the housing plate. The friction remains low even if there is relative motion between the two layers because of the ball bearings.

3.1.4. Polycarbonate Tube

In this prototype, the pump tube and its base are made of polycarbonate, as shown in Figure 3-8. Polycarbonate is a transparent, strong, and stiff thermoplastic material with outstanding impact resistance. Toughness and optical clarity make polycarbonate ideal for a wide variety of applications including machine guards, indoor and outdoor signs, architectural glazing, face shields, skylights, and point-of-purchase displays [48]. Polycarbonate rods and plates are also easy to machine and have excellent dimensional stability. The fact that the pump tube is transparent makes it easier for troubleshooting and showcasing the concept of the proposed mechanism. For this prototype, the pump tube is of ID 3.25”, OD 3.5” and 18” long.

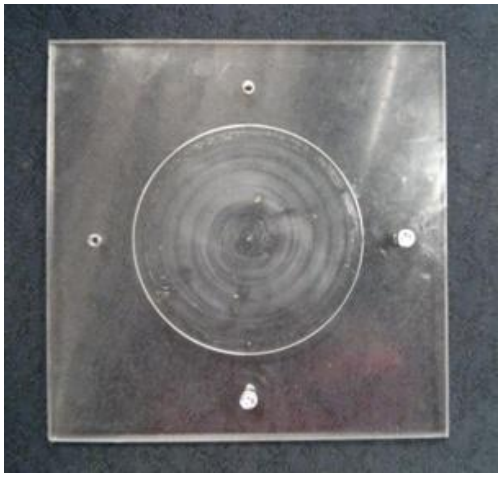

Figure 3-8. Polycarbonate Tube Base

The other end of the tube is sealed with a cap pair, as shown in Figure 3-1. The pair consists of a male part with external thread and a female part with internal thread. Threads are created according to Unified Thread Standard (UTS) [44] because it is easy to be modelled in CAD programs. It is the main standard for bolts, nuts, and a wide variety of other threaded fasteners used in United States and Canada. The male cap is glued to the ouside wall of the pump tube at its end, and the female counterpart could be screwed onto the male part. This threaded pair makes it easy to assemble and disassemble the pump prototype. Same as the transmission roller, the cap pair is also 3D printed with ABS because of the complicated shape of the threads. To make a fluid-tight seal between this pair, PTFE tape or Teflon tape is used.

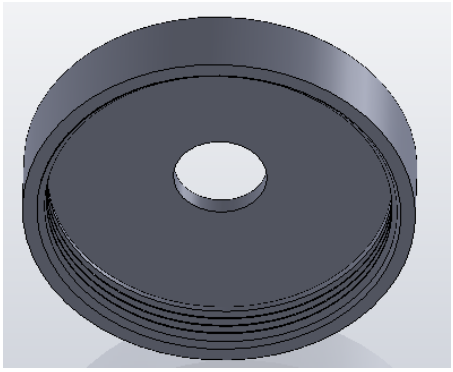

(a) Female End Cap

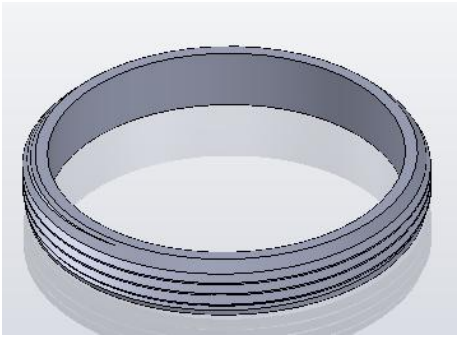

(b) Male End Cap

Figure 3-9. End Cap Pair

3.1.5. Check Valves

Check valves are mechanical valves that permit gases and liquids to flow in only one direction. Cracking pressure of a check valve is the minimum upstream pressure at which the valve will operate. In this prototype, it also affects how much pressure this pump prototype could generate since pressure in PDPs is generated due to resistance to the flow. The purpose of building this prototype is to validate the functionality of the transmission roller, thus the cracking pressure of the check valves should be chosen as low as possible. IPEX VB ball check valves are selected for the prototype, as shown in Figure 3-10. The body material is PVC with Viton seals and the size is 3/4”. The cracking pressure for this valve is just a few psi.

Figure 3-10. IPEX VB Ball Check Valves

National Pipe Thread Taper (NPT) is a U.S. standard for tapered threads used on threaded pipes and fittings. The end connection for this valve is female NPT threaded. A male NPT threaded connection could be attached to its end. To make a fluid-tight seal between the ball check valve and its connections, PTFE tape or Teflon tape is used.

Usually ball check valves have better performance when put in the vertical direction [45] in terms of reverse flow velocity and water hammer effect. In this project, since the output pressure is negligible and the flow rate is relatively low, it won't affect the performance of the check valve much if they are placed horizontally.

3.2. Prototype Overview

The fabricated prototype is shown in Figure 3-11. Two hoses are connected to the check valves. One hose is connected to the inlet and the other is connected to the outlet. Lubricant has been used during assembly when dealing with tight clearances.

Figure 3-11. Pump Prototype

Note that the prototype design is not the final production design and they might be different in the following ways. Firstly, the pump structure is different. In order to simply and economize the prototype fabrication process, the diaphragm is taken out to avoid dealing with oil which complexes the process. For the final production design, there will be a diaphragm separating process fluid from the outer oil environment. Transmission roller will also be immersed in an oil chamber and thus the seals on the plunger in the current design will be redundant. The arrangement of the check valves might be different too. Currently the inlet check valve is located on one side of the pump tube. However, this might be impractical in reality because of the space constraint. Instead of using one 3/4" valve, more smaller valves could be put around the pump tube acting as inlets for the final production design and yet have the equivalent area for pump inlet. Secondly, the pressure rating for the final product is different from the prototype. The output pressure is negligible while the output pressure for a slurry deep application might be up to 1000 psi. The customized parts should be machined using metal instead

of 3D printed with ABS, such as transmission roller. The other parts should also be upgraded to their counterparts that could handle larger pressure. For example, a larger cracking pressure should be chosen for check valves.

Chapter 4.
Pump Design Analysis

Different analysis has been carried out in order to fully assess the feasibility of the transmission roller design. A very important parameter for measuring its performance is the efficiency. A mathematical method of calculating the efficiency of the transmission roller using experimental data is introduced. Then the mathematical model built is used to estimate the largest loading force that is applied on the transmission roller in the prototype, and the minimum power needed to actuate the pump prototype in an ideal situation.

The pump prototype is built to demonstrate its functionality. For a production design, a higher output pressure for deep well applications is expected and the final production transmission roller must be able to withstand that pressure. A stress analysis for a production version of the transmission roller made of stainless steel is carried out using ANSYS and suggestions for modifications are made based on the results.

4.1. Transmission Roller Efficiency Estimation

Generally speaking, pump efficiency could be defined as the ratio of power output by the pump and power input to the pump. Ideally, a pump should be 100% efficient, but this is not achievable due to energy losses during power transmission. The two main efficiencies that make up an overall pump efficiency are torque efficiency and volumetric efficiency. “Torque efficiency describes the power losses that result from fluid shear and internal friction. Volumetric efficiency describes the power losses that result from internal leakage and fluid compressibility ” [51]. In this prototype, torque efficiency mainly depends on two friction losses. One is the friction loss due to the sealings around the plunger. The other loss is due to the friction between the ball bearings and tracks. Many attempts have been made to model pump efficiency with some degree of accuracy.

Until now, there isn't an accurate way to predict pump efficiency characteristics in an a priori way, therefore, experimental coefficients or data collected from tests are used to help predict efficiency [51]. To estimate the efficiency of the transmission roller, experimental data is also used in this project.

The efficiency of the transmission roller makes up a major part for torque efficiency and friction loss is the major energy loss for the transmission roller. Equations for the friction force between the steel ball bearings and the ABS plunger tracks are developed first. Using the data collected from the tests, including average motor power and motor rotary speed, the efficiency of the transmission roller is estimated. This estimation method is also used in later chapters to calculate the efficiency of the prototype transmission roller and the production version.

One pump cycle is chosen to carry out the analysis. During this cycle, the pump has gone through a suction stroke and a discharge stroke, while the motor has rotated 180º. Figure 4-1 presents the shape of one track, unwrapped to plane, that ball bearings roll on within this cycle. Forces applied on the bearing by the track are also shown. The bearing is considered as a mass point in this model for simplification.

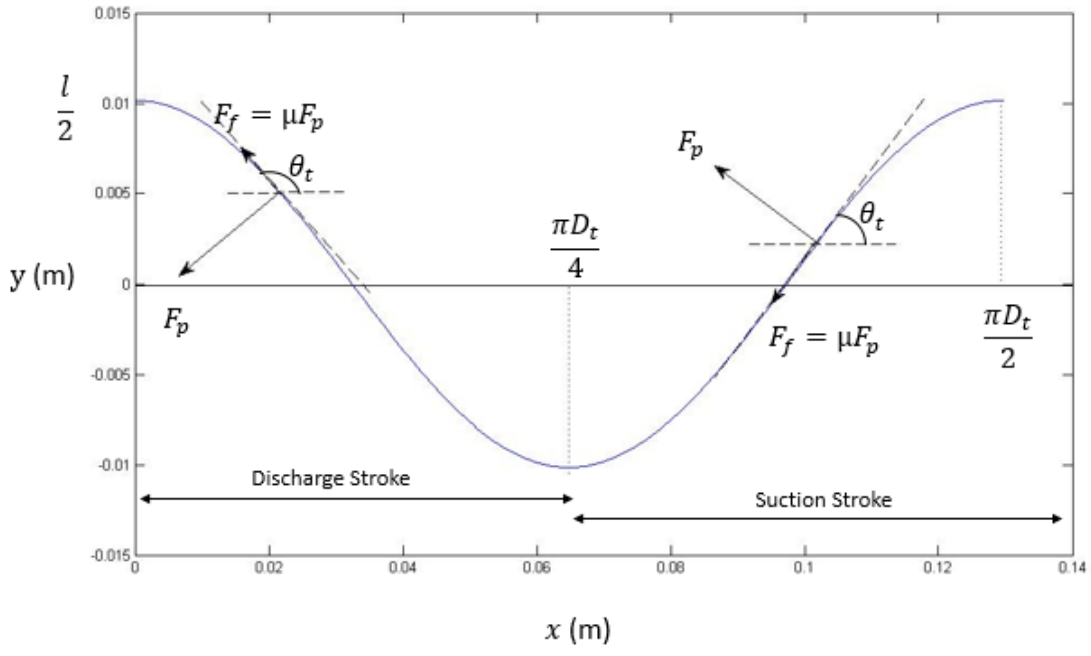

Figure 4-1. Shape of One Track Unwrapped to Plane

The track is in the shape of a sine curve. Since there are two cycles of the sine curve engraved on the outer surface of the plunger, the cycle length equals to half of the circumference of the plunger cross section. Eq. 2.11 which describes the curve is rewritten here.

$$y = \frac{l}{2}\sin\left(\frac{4}{D_t}x + \frac{\pi}{2}\right) \tag{4.1}$$

where D_t is the diameter of the plunger for the track part and l is the amplitude of the curve shape. θ_t in the graph is the gradient angle of the tangent line of the curve. The relationship between this angle and the gradient could be expressed as below.

$$\dot{y} = \tan\theta = \frac{2l}{D_t}\cos\left(\frac{4}{D_t}x + \frac{\pi}{2}\right) \tag{4.2}$$

It could be observed that the function of $\dot{y}$ has the following characteristics, which will be applied later in this chapter.

$$\dot{y}\left(x + \frac{\pi D_t}{4}\right) = -\dot{y}(x) \tag{4.3}$$

$$\dot{y}^2\left(x + \frac{\pi D_t}{4}\right) = \dot{y}^2(x) \tag{4.4}$$

$$\dot{y}\left(\frac{\pi D_t}{4} - x\right) = \dot{y}(x) \tag{4.5}$$

F_p is the normal force exerted by the track onto the bearing. The direction of F_p is always perpendicular to the tangent line of the track curve. As illustrated in Figure 4-1, the ball bearing experiences a downward F_p when rolling down the track. This is because the bearing is uplifting the plunger at the moment while the pump is in a discharge stroke. In contrary, when the bearing is rolling up the track, F_p becomes an upward force while the bearing is pushing down the plunger incurring a suction stroke of the pump.

F_f is the friction force exerted by the track onto the bearing. The direction of F_f is always the opposite of the moving direction and it is parallel to the tangent line of the

track curve. μ stands for coefficient of friction between the bearing and the plunger track. Thus,

$$F_f = \mu F_p \tag{4.6}$$

In order to estimate the friction loss, the expression for F_p is needed. It is already known that the direction of F_p is perpendicular to the curve, pointing downwards during discharge strokes and pointing upwards during suction strokes. It could be deduced that F_p gradually increases as the absolute value of the curve gradient becomes larger, or as the track becomes steeper. When track becomes steeper, the vertical velocity and acceleration of the plunger is bigger which would require a larger support force or a pressing force from the bearings. It could also be deduced that F_p equals to zero both at highest point and lowest point of the track because the force changes its direction at those points. Thus, the deduced pattern of F_p is shown in Figure 4-2.

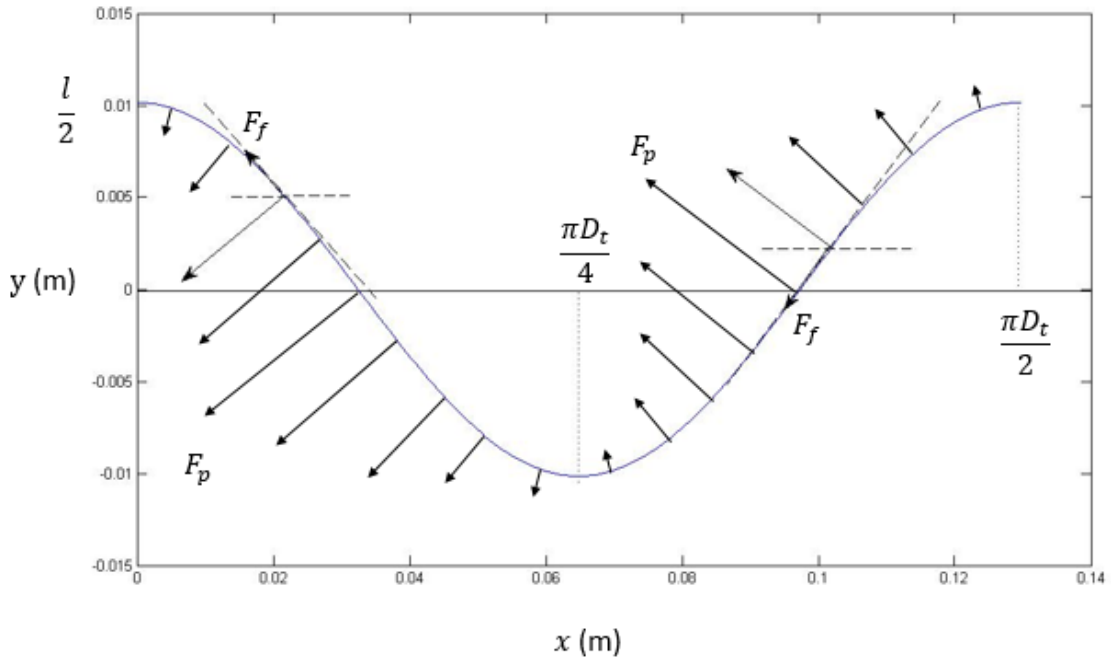

Figure 4-2. Pattern of F_p

Based on the above analysis, an assumption is made that F_p could be expressed in the form as below,

$$F_p = Asin\left(\frac{4}{D_t}x\right), x\epsilon[0, \frac{\pi D_t}{4}] \tag{4.7}$$

$$F_p(\mathrm{x} + \frac{\pi \mathrm{D_t}}{4}) = F_p(\mathrm{x}) \tag{4.8}$$

where A is constant which later will be deduced. A graph of F_p is shown in Figure 4-3.

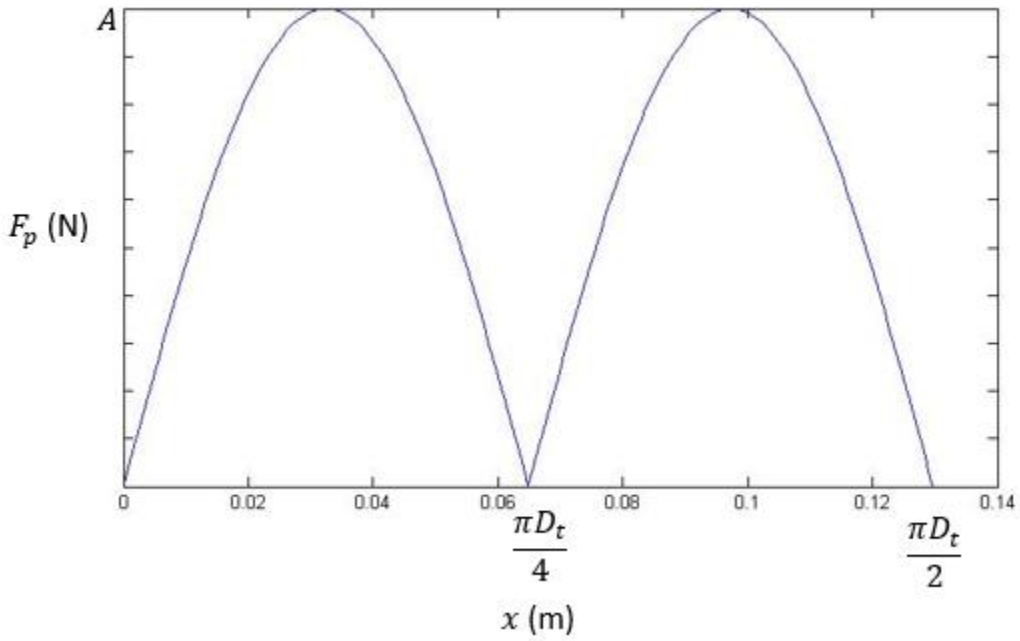

Figure 4-3. Amplitude Pattern for Force $\mathbf{F_p}$

F_p has the property of symmetry of a sine curve

$$F_p(\frac{\pi \mathrm{D_t}}{4} - \mathrm{x}) = F_p(\mathrm{x}), x\epsilon[0, \frac{\pi D_t}{4}] \tag{4.9}$$

In order to obtain the value of A, torques applied on the bearings are analysed. The motor applies a torque to the revolver that accelerates its rotary speed. Another torque is applied on the revolver by the plunger through F_p and F_f that decelerates its rotary speed. When the pump achieves a balanced and stable working status, the revolver should not experience a change of its rotary speed over a time period. Thus the accelerating torque and the decelerating torque should be equivalent.

The accelerating torque provided by motor τ_{mot} could be calculated from experimental data, using the motor power P_{mot} and motor rotary speed ω.

$$\tau_{mot} = \frac{P_{mot}}{\omega} \tag{4.10}$$

The average decelerating torque τ_d is provided through F_p and F_f. τ_d over one cycle could be expressed as below.

$$\tau_d = \frac{1}{\frac{\pi D_t}{2}}\left[\int_0^{\frac{\pi D_t}{4}} 4\left(F_p \sin\theta - F_f \cos\theta\right) D_t \, dx + \int_{\frac{\pi D_t}{4}}^{\frac{\pi D_t}{2}} 4\left(F_p \sin\theta + F_f \cos\theta\right) D_t \, dx\right] \tag{4.11}$$

There are 4 bearings in total in this prototype which explains the coefficient 4 in the equation.

Now we simplify the Eq. 4.11. Using trigonometry, it could be easily obtained when $x \in \left[0, \frac{\pi D_t}{4}\right]$

$$\sin\theta = \frac{-\tan\theta}{\sqrt{\tan^2\theta + 1}} \tag{4.12}$$

$$\cos\theta = \frac{-1}{\sqrt{\tan^2\theta + 1}} \tag{4.13}$$

When $x \in \left[\frac{\pi D_t}{4}, \frac{\pi D_t}{2}\right]$

$$\sin\theta = \frac{\tan\theta}{\sqrt{\tan^2\theta + 1}} \tag{4.14}$$

$$\cos\theta = \frac{1}{\sqrt{\tan^2\theta + 1}} \tag{4.15}$$

Using the above trigonometry properties, Eq. 4.2, Eq. 4.6 and Eq. 4.7, it could be obtained

$$\tau_d =$$

$$\frac{1}{\frac{\pi D_t}{2}}\left[\int_0^{\frac{\pi D_t}{4}} 4\left(Asin\left(\frac{4}{D_t}x\right)\frac{-\tan\theta}{\sqrt{\tan^2\theta+1}} - \mu Asin\left(\frac{4}{D_t}x\right)\frac{-1}{\sqrt{\tan^2\theta+1}}\right) D_t\, dx + \right.$$

$$\pi Dt 4\pi Df 24 Asin 4 Dtx \tan\theta \tan 2\theta + 1 + \mu Asin 4 Dtx 1 \tan 2\theta + 1 Dt\, dx$$

$$= \frac{8A}{\pi}\left[\int_0^{\frac{\pi D_t}{4}} sin\left(\frac{4}{D_t}x\right)\frac{\mu-\dot{y}}{\sqrt{\dot{y}^2+1}}dx + \int_{\frac{\pi D_t}{4}}^{\frac{\pi D_t}{2}} sin\left(\frac{4}{D_t}x\right)\frac{\mu+\dot{y}}{\sqrt{\dot{y}^2+1}}dx\right] \quad (4.16)$$

Using Eq. 4.3, Eq. 4.4 and Eq. 4.8, it could be obtained

$$\tau_d = \frac{8A}{\pi}\left[\int_0^{\frac{\pi D_t}{4}} sin\left(\frac{4}{D_t}x\right)\frac{\mu-\dot{y}}{\sqrt{\dot{y}^2+1}}dx + \int_0^{\frac{\pi D_t}{4}} sin\left(\frac{4}{D_t}\left(x+\frac{\pi D_t}{4}\right)\right)\frac{\mu+\dot{y}\left(x+\frac{\pi D_t}{4}\right)}{\sqrt{\dot{y}^2\left(x+\frac{\pi D_t}{4}\right)+1}}d\left(x+\frac{\pi D_t}{4}\right)\right]$$

$$= \frac{16A}{\pi}\int_0^{\frac{\pi D_t}{4}} sin\left(\frac{4}{D_t}x\right)\frac{\mu-\dot{y}}{\sqrt{\dot{y}^2+1}}dx \quad (4.17)$$

Using Eq. 4.5 and Eq. 4.9, the expression for τ_d could be developed as

$$\tau_d = \frac{16A}{\pi}\left[\int_0^{\frac{\pi D_t}{8}} sin\left(\frac{4}{D_t}x\right)\frac{\mu-\dot{y}}{\sqrt{\dot{y}^2+1}}dx + \int_{\frac{\pi D_t}{8}}^{\frac{\pi D_t}{4}} sin\left(\frac{4}{D_t}x\right)\frac{\mu-\dot{y}}{\sqrt{\dot{y}^2+1}}dx\right] =$$

$$\frac{16A}{\pi}\left[\int_0^{\frac{\pi D_t}{8}} sin\left(\frac{4}{D_t}x\right)\frac{\mu-\dot{y}}{\sqrt{\dot{y}^2+1}}dx + \int_{\frac{\pi D_t}{8}}^{0} sin\left(\frac{4}{D_t}\left(\frac{\pi D_t}{4}-x\right)\right)\frac{\mu-\dot{y}\left(\frac{\pi D_t}{4}-x\right)}{\sqrt{\dot{y}^2\left(\frac{\pi D_t}{4}-x\right)+1}}d\left(\frac{\pi D_t}{4}-x\right)\right]$$

$$= \frac{32A}{\pi}\int_0^{\frac{\pi D_t}{8}} sin\left(\frac{4}{D_t}x\right)\frac{\mu-\dot{y}}{\sqrt{\dot{y}^2+1}}dx \quad (4.18)$$

Now an equation could be written based on the fact that the accelerating motor torque is equivalent to the average decelerating torque so that the value of A could be obtained.

$$\tau_{mot} - \tau_d = \frac{P_{mot}}{\omega} - \frac{32A}{\pi}\int_0^{\frac{\pi D_t}{8}} sin\left(\frac{4}{D_t}x\right)\frac{\mu-\dot{y}}{\sqrt{\dot{y}^2+1}}dx = 0 \quad (4.19)$$

$$\mathrm{A} = \frac{\pi P_{mot}}{32\omega \int_0^{\frac{\pi D_t}{8}} sin\left(\frac{4}{D_t}x\right) \frac{\mu - \dot{y}}{\sqrt{\dot{y}^2+1}} dx} \tag{4.20}$$

Now F_p is known, the friction loss of the transmission roller over one pump cycle W_f could be given by

$$W_f = 4 \int_0^{\frac{\pi D_t}{2}} F_f \sqrt{1+\dot{y}^2}\, dx \tag{4.21}$$

Like simplifying the expression for τ_d, similar properties of F_p and $\dot{y}$ are used to simplify the expression for W_f.

$$W_f = 4 \int_0^{\frac{\pi D_t}{2}} \mu F_p \sqrt{1+\dot{y}^2}\, dx = 8 \int_0^{\frac{\pi D_t}{4}} \mu F_p \sqrt{1+\dot{y}^2}\, dx$$

$$= 16\mu\mathrm{A} \int_0^{\frac{\pi D_t}{8}} sin\left(\frac{4}{D_t}x\right) \sqrt{1+\dot{y}^2}\, dx \tag{4.22}$$

The value of W_f could be obtained from Eq. 4.22. Using the data collected from testing, the transmission efficiency of the transmission roller η_t could be given by

$$\eta_t = 1 - \frac{W_f}{W_{mot}} = 1 - \frac{W_f}{P_{mot}T} \tag{4.23}$$

where W_{mot} is the power provided by the motor over one pump cycle and T is the time for one pump cycle, which includes the time of one discharge stroke and one suction stroke.

The above method for estimation of the transmission efficiency of the transmission roller is applied for the prototype transmission roller and the final production one in Chap. 5.

4.2. Loading Force Estimation

It is important to know what conditions the transmission roller will be working with during the tests. An estimation of the loading force that is applied on the transmission roller in the prototype is presented in this section.

As illustrated previously, the plunger moves in the vertical direction in a reciprocating manner as shown in Figure 4-4. Eq. 2.13 which expresses the plunger displacement z in terms of time t is rewritten here.

$$z = \frac{l}{2} sin\left(2\omega t - \frac{\pi}{2}\right) \tag{4.24}$$

The velocity and the acceleration of the plunger could be deduced as below.

$$\dot{z} = l\omega \, cos(2\omega t - \tfrac{\pi}{2}) \tag{4.25}$$

$$\ddot{z} = -2l\omega^2 \, sin(2\omega t - \tfrac{\pi}{2}) \tag{4.26}$$

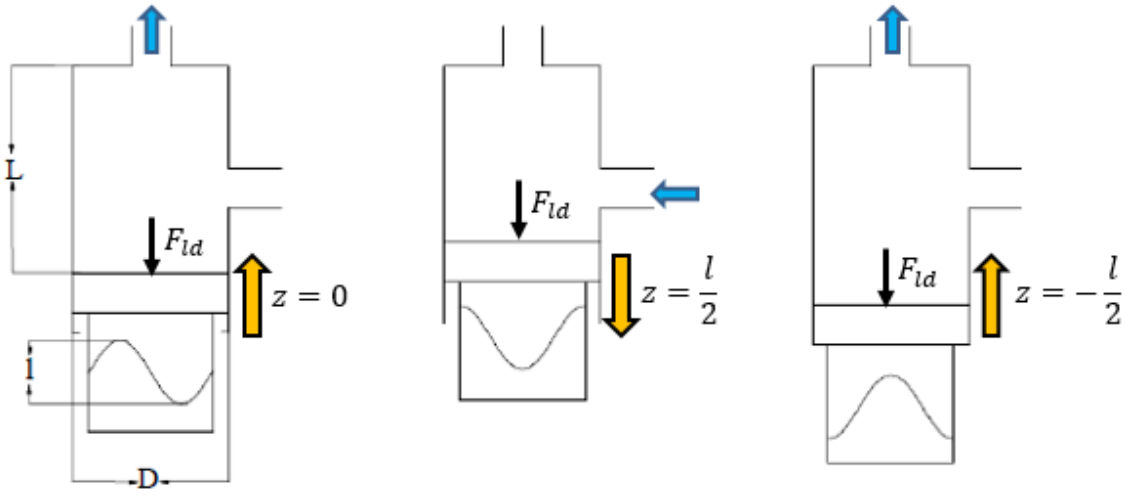

(a) Middle of Discharge Stroke (b) Start of Suction Stroke (c) Start of Discharge Stroke

Figure 4-4. Movement of the Plunger in the Transmission Roller

The cracking pressure of the check valves is negligible in this prototype, thus the acceleration of transferred fluid a_f is equal to the acceleration of the transmission roller $\ddot{z}$.

$$a_f = \ddot{z} \tag{4.27}$$

Applying Newton's second law on the transmission roller, it could be obtained

$$F_{fld} - m \times g = m \times a_f \tag{4.28}$$

where F_{fld} is the force applied on the fluid by the transmission roller and m is the mass of the fluid in the pump chamber. m is given by

$$m = \rho \times \pi \times \left(\frac{D}{2}\right)^2 \times (L - z)$$

$$= \frac{1}{4}\pi\rho D^2(L - z) \tag{4.29}$$

where D is diameter of the plunger and L is height of the pump chamber when the plunger of the transmission roller is in the middle of its stroke, i.e. when $z = 0$. Apply the Newton's first law on F_{fld}, it is obtained

$$F_{ld} = F_{fld} = \frac{1}{4}\pi\rho D^2(L - z) \times (g - 2l\omega^2 \, sin(2\omega t - \frac{\pi}{2})) \tag{4.30}$$

where F_{ld} is the load force applied on the transmission roller.

Eq. 4.30 illustrates how the loading force changes when the pump prototype is working. The maximum load force for the prototype is also calculated using this equation later. The loading force for the prototype is expected to be small because the output pressure is negligible. However, for the final production design, the output pressure could be up to 1000 psi according to Toyo's expectation. In that case, it is important to check whether the transmission roller is able to withstand that much pressure without structural failures.

4.3. Stress Analysis for the Production Design

For slurry applications, there is usually a requirement for the output pressure and it could be up to 1000 psi. For this reason, the transmission roller would be produced using metal material in the final design such as 316 SS, instead of being 3D printed with ABS plastic. For the production design, it is important to see how much pressure or load force the transmission roller could withstand. It is also very helpful to see how the load force is distributed into different areas of the transmission roller. In this section, a structural and design analysis of the transmission roller made of stainless steel is presented. Suggestions for modification of the current transmission roller design are made based on the analysis results. ANSYS is used to perform finite element analysis.

To accomplish this, a static structure FEA of the transmission roller is performed. The original CAD model used is the conceptual one described in Chapter 2. Only half of the transmission model is used in the analysis because of its symmetric structure. The model is processed to remove non-essential features to improve meshing quality and save computer time. For this analysis, the load pressure is set as 1000 psi, or load force 36.9 kN for the provided CAD model. However, the load pressure or force should be set differently for applications with different head requirements. The result indicated weaknesses in the current design around the bearings and at the bottom of the revolver.

4.3.1. Preprocessing

For geometry simplification, the revolver and the plunger have been sliced and de-featured to create a geometry that is easier to mesh. The fillet between the shaft and bottom plate is removed using Face Delete, as shown in Figure 4-5. There are two small pins protruding from the plunger main body which tend to interfere with the accuracy of this analysis. The pins are sliced and thus separated from the plunger.

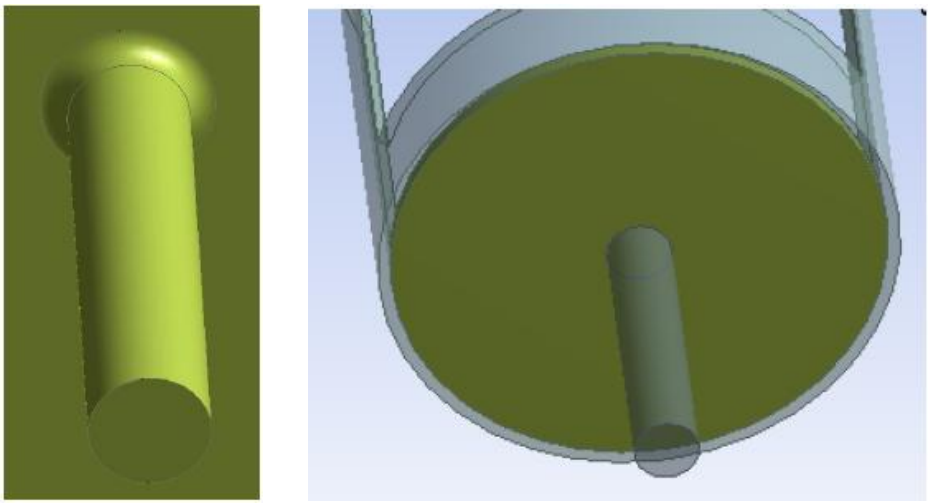

a) Original Shaft b) Sliced and De-featured Shaft

Figure 4-5. Sliced and De-featured Shaft

The full structure is also sliced along lines of symmetry to reduce number of elements and thus reduce computing time.

4.3.2. Connections and Contacts

Each contact is defined between two bodies. Some of the contacts are defined as frictional with a frictional coefficient. Most contacts are defined as bonded which means that the bodies can't move relatively to each other and are fixed together. The contact definitions are shown in Figure 4-6. The bearings are located in the middle of the stroke for this analysis

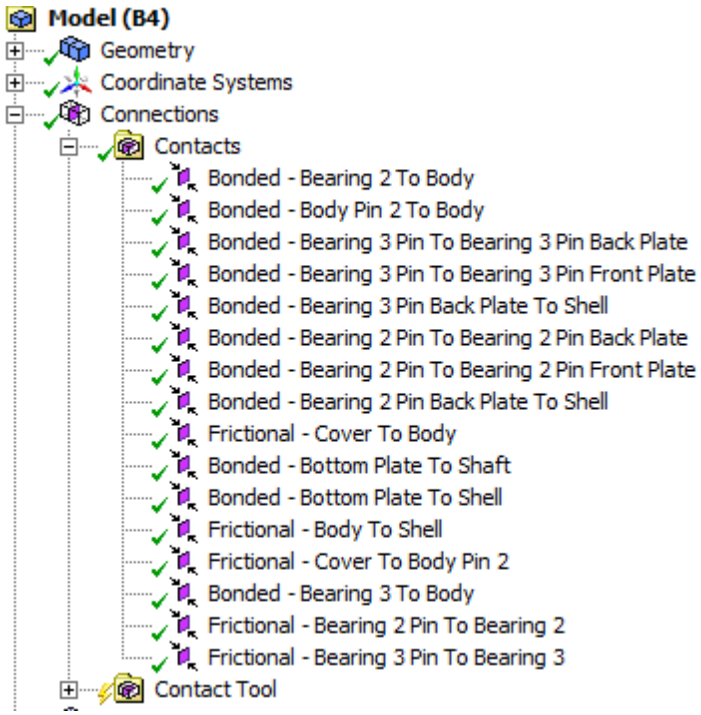

Figure 4-6. Contact Definitions for the model

Tuning is often required for contact definitions. The frictional contacts between the bearings and pins are nonlinear and play an important role for the analysis. Therefore, more advanced penetrated-based tunings are applied.

4.3.3. Meshing and Boundary Conditions

Since the geometry of the device is irregular and the automatically generated mesh is of poor quality, meshing control is used in order to obtain a better mesh by increasing the density of elements in important areas. Contact sizing is used to refine the contact region and smaller elements are set for the regions of concern. Body sizing is applied to the plunger part as it has irregular geometry. Face sizing and edge sizing are applied on the lower part of the revolver, which suffers more stress and has larger deformation comparing to other parts. Edge sizing is suitable for the rectangular revolver bottom because it has regular shape and face sizing is more suitable for the quarter circle revolver bottom for its nonlinear geometry shape. This meshing sizing process increased the number of elements from 2576 to 3379. The meshing control was tuned until the results have converged.

56kN force is generated by the pump during operation. For the hal model, only half of this force is applied. Standard earth gravity is applied to the model to simulate the self-body force. The shaft of the revolver si fixed at the bottom surface as no rotation force could be applied in the static analysis. The cover is supposed to lock the plunger from rotating and thus also has a fixed support. The Transmission roller is symmetric and the displacement along the normal of symmetric plane is zero. Therefore, displacement controls are applied along the cut surface to ensure the displacement along the symmetric plane is zero.

Figure 4-7. Boundary Control of the Transmission Roller

4.3.4. Results

The total force applied on the surface of the body is 18.5 kN, half of 36.9 kN, since the model is cut in half due to symmetry. The resultant stress profile is shown in Figure 4-8 and Figure 4-9.

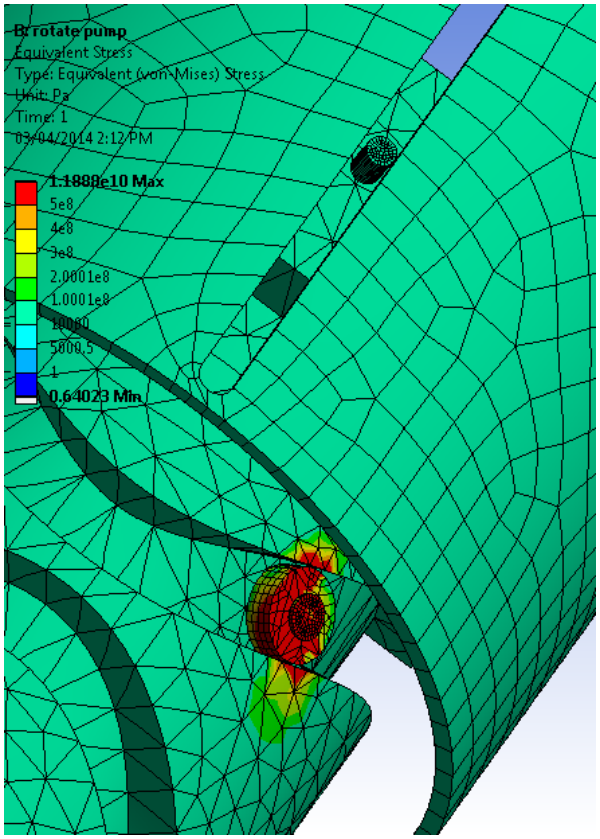

Figure 4-8. Stress in Bearing Area of the Middle Position Half Model

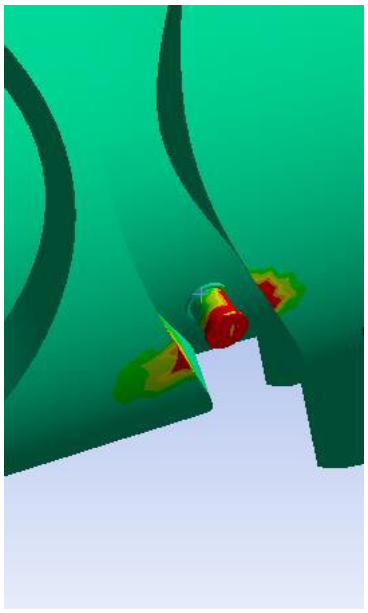

Figure 4-9. Stress in Pin Back Area of the Middle Position Half Model

As expected, the load force is ultimately transferred to the bearing. Since the contact area between the bearing and the groove is relatively small, the stress concentration is the largest in this area. The stress in this area is more than ten times compared to other parts. This indicates the tracks will be subject to a lot of wear when the pump is working. The stress on the area around the back of the pin which supports bearings is also relatively large. This is because the pin undergoes bending when the bearing is pressed down by the plunger, thus the area where the back plate pin connects to the revolver experiences large stress.

Because the proposed mechanism has to sustain up to 36.9 kN of force, a safety factor analysis is useful to determine whether the structure is capable of sustaining such loads. The safety factor plot, as shown in Figure 4-10, indicates that the lower plate of the revolver and the areas around the bearings in their current shapes are the weakest parts of this design and suffer more stress when the pump is working. Since the safety factors for these areas are below 1, it is indicated that these areas may not be capable of withstanding the rated load.

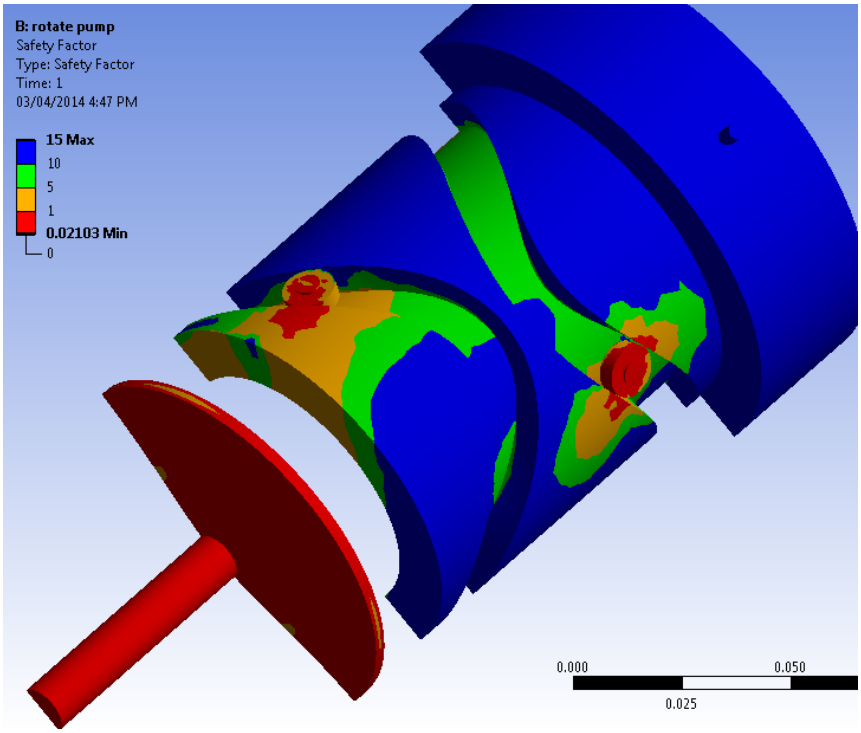

Figure 4-10. Safety Factor Plot

For future work, these areas with safety factors below 1 should strengthen the structure by increasing the contact areas to decrease the pressure, or by increasing the thickness of the plate areas. The improved model should be put back into the ANSYS model and analysed again until the safety factors are all above 1 in this model. Another way is to update the material from using stainless steel to titanium. Titanium is three times stronger than stainless steel, but it will also increase the production cost.

Chapter 5.
Performance Test

In this chapter, the pump prototype is tested with water to demonstrate the functionality of the transmission roller. Information about the test setup, parameters measurement and results are introduced. Most of the procedures are based on ANSI/HI 6.6-1994 Reciprocating Pump Tests [52]. This standard provides uniform procedures for hydrostatic, hydraulic and mechanical pump performance testing and for recording of the test results of reciprocating pumps. Relevant experimental data is used later to assess the performance of the pump prototype and predict the performance of the final production pump.

5.1. Test Setup

The pump prototype introduced in Chap.3 is placed horizontally. A bench power supply PSC-520 from Circuit-test Electronics is used as the electricity source for the pump motor. This power supply has a single output and LCD voltage and current display with 4 digits. The value of the voltage and current will be recorded for calculation of the motor power. Two water tanks are used. One is used as an inlet water reservoir, while the other one is used as the outlet water reservoir. The outlet tank dimension is 39.0 cm (length) X 29.5 cm (width) X 33.0 cm (height). Figure 5-1 is a representation of the instrumentation.

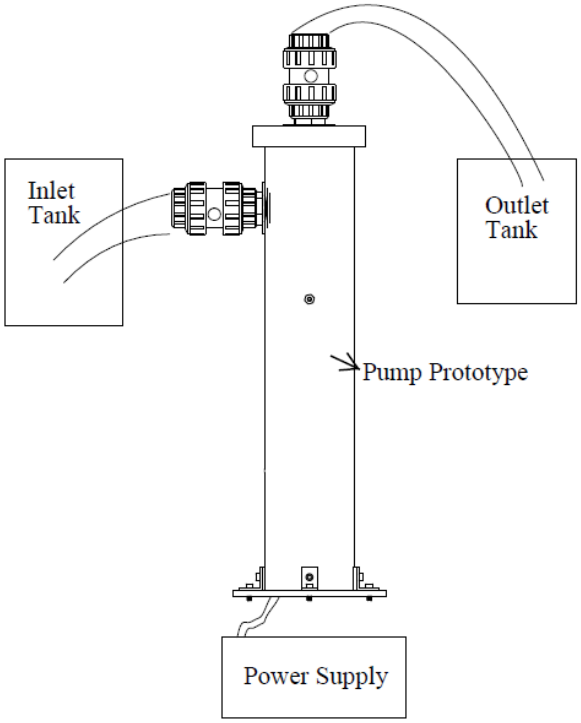

Figure 5-1. Instrumentation of the Prototype Test

It is observed that the prototype is working fine and the transmission roller is functioning well as expected. However, some issues are also spotted through running the prototype. It could be observed that air is leaked into the pump chamber. The air is mainly leaked in through the connection at the inlet and outlet and the connection of the end cap to the pump tube. These connections are made mostly watertight through NPT threads and Teflon tape. However, they are not airtight. With air inside the pump chamber, more energy is applied to compress and decompress the leaked air instead of pumping water, which decreases the efficiency of the pump. This air leakage wouldn't be an issue for the final production design because most of the connections would be welded and thus airtight. The transferred fluid would also be separated by the diaphragm which guarantees zero leakage.

Another issue spotted is the large friction between the U-cup around the plunger and the pump tube. As mentioned in Chapter 2, the diaphragm is taken out of this design for the simplification of prototype building. Though this modification doesn't get in the way of demonstrating the concept and the function of the transmission roller, it does put

a heavy burden on the sealing between the pump chamber and the motor section. With the diaphragm and thus the oil reservoir absent, the sealing around the plunger needs to tight enough preventing the leakage of water into the motor area. A big friction is incurred without oil lubrication between the U-cup and the pump tube. This also decreases the efficiency of the pump prototype. For the final production design, the sealing doesn't need to be as tight since both sides of the plunger are bathed in an oil reservoir and friction is much smaller with oil lubrication.

5.2. Parameters Measurement and Deduction

Experimental data has been collected during the test for assessment of the pump prototype performance. Using this data, the transmission efficiency of the transmission roller and the overall efficiency of the pump prototype is calculated.

The total time period length for the test Δt is 130s. During this time period, there are 166 pump cycles in total and the water level in the outlet reservoir has an increase of 19 cm. It is illustrated in this section how these parameters are measured and used to assess pump performance.

5.2.1. Pump Speed (n)

The revolution counter and timer method introduced in ANSI/HI 6.6-1994 [52] is used here to measure the pump speed. Pump speed is the number of pump cycles per time unit. This method involves the counting of the number of pump cycles over an interval of time. A handheld counter and a stopwatch are used and the timing interval is chosen as two minutes. In this test, the number of revolutions are counted manually and the time is measure by the timing app in LG Nexus 4 E960. There are other methods measuring pump speed using tachometers, frequency-responsive devices and stroboscopes. Compared with those methods, the revolution counter and timer method is more cost efficient and budget wise. The major disadvantage of this method is that accuracy is compromised due to inexact synchronization of counter and timer. However, accuracy is not needed for this test. The pump speed is thus given by

$$n = \frac{N}{\Delta t} = \frac{166\ cycle}{130s} = 1.28\ cycle/s \tag{5.1}$$

where N is the number of pump cycles completed within the testing time period.

5.2.2. Capacity (Q)

Capacity Q is the quantity of liquid actually delivered per unit of time. There are different ways and instruments to measure it, such as displacement type meters, head type rate meters and venture meters. The instruments that measure capacity could be classified into two groups. The first measures batch quantity and the other primarily measures rate of flow.

In this test, a cost-effective way is used since the accuracy of the test results is not the priority. The volume of the fluid that is pumped into reservoir during a certain time period is used to calculate capacity Q. The volume of the fluid could be measured by fluid level increase in the outlet reservoir. This level increase is measured by a measuring tape with a scale division of 0.1 cm. Capacity Q equals the volume divided by the time period.

During the testing time period Δt 130s, the water level in the outlet reservoir has an increase Δh of 19.0 cm. A_{r} is the area of the horizontal cross section of the outlet reservoir. Capacity Q is given by

$$Q = \frac{A_r \Delta h}{\Delta \mathrm{t}} = 2.665\ GPM \tag{5.2}$$

5.2.3. Pump Output Power (P_W)

The total differential pressure p_H is the measure of the pressure increase imparted to the liquid by the pump and is therefore the difference between the total discharge pressure p_{out} and the total suction pressure p_{in}:

$$p_H = p_{out} - p_{in} = \rho g \left[\frac{(v_{out})^2}{2g} + Z_{out}\right] - \rho g \left[\frac{(v_{in})^2}{2g} + Z_{in}\right] \tag{5.3}$$

where Z_{out} is the elevation head of the outlet and Z_{in} is the elevation head of the inlet. Elevation heads are referred to the centreline of the pump inlet from which all elevations are measure. Z_{out} is measured to be 13.0 in and $Z_{in} = 0$. v_{out} is the flow velocity at the outlet and v_{in} is the flow velocity at the inlet. $v_{in} = 0$ and v_{out} is given by

$$v_{out} = \frac{Q}{\pi(\frac{D_v}{2})^2} \tag{5.4}$$

where D_v is the diameter of the check valve at the outlet. As introduced in Chap. 3, the diameter of the check valve is 3/4".

Using the calculated value of the capacity Q in Eq. 5.2 and the parameters mentioned above, the pump output power P_W could be calculated as below.

$$P_W = Q \times p_H = Q \times \rho g \left\{ \frac{\left[\frac{Q}{\pi\left(\frac{D_v}{2}\right)^2}\right]^2}{2g} + Z_{out} \right\} = \rho g Q \left(\frac{8Q^2}{\pi^2 {D_v}^4 g} + Z_{out} \right) = (0.029 +$$

$$0.544\,W = 0.573\,W \tag{5.5}$$

5.2.4. Motor Power ($\mathbf{P_{MOT}}$)

Electric power of a motor could be calculated using the equation below.

$$P_{MOT} = \eta_m UI \tag{5.6}$$

where η_m is the motor efficiency, U is the voltage provided by the power source and I is the current provided. In this case, the motor efficiency η_m is considered to be 79.5% according to the motor specifications.

Data for voltage and current is displayed on the screen of the power supply in a real-time manner. Through testing, it is observed that both the voltage and current are constantly changing when the pump is working. The reason is that the pump loading keeps changing as water is pumped in and out of the chamber, suggested by Eq. 4.30. In order to calculate pump efficiency, an average motor power needs to be estimated.

Thus, a sample of the current and voltage data is taken which lasts 10 s. During this 10 s, there are about 15 pumping cycles. The number of cycles is enough for calculation of average power. Data which is collected from the sample is displayed in Appendix B, which includes both the voltage and current data. Graphs are drawn for both parameters, as shown in Figure 5-2 and Figure 5-3.

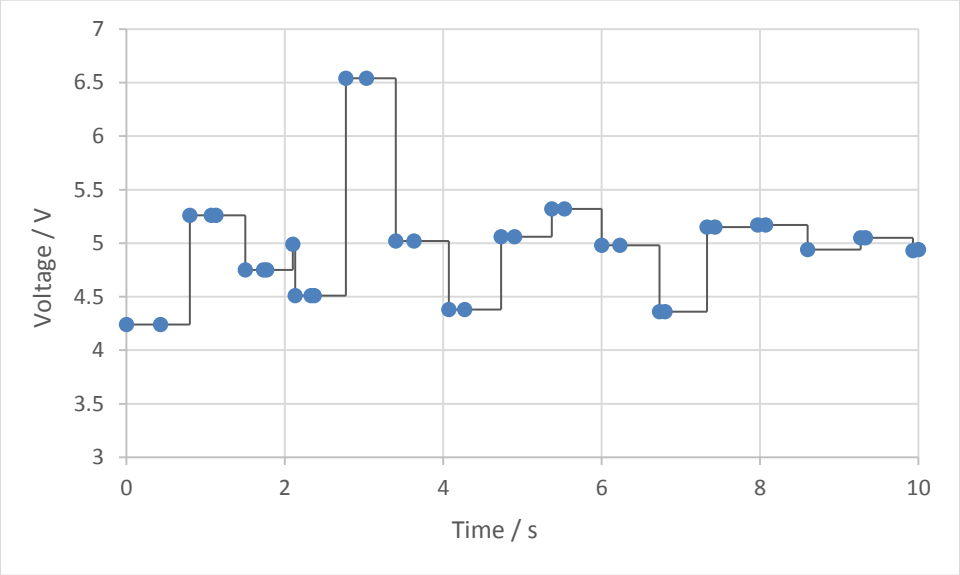

Figure 5-2. Voltage Provided by the Power Supply

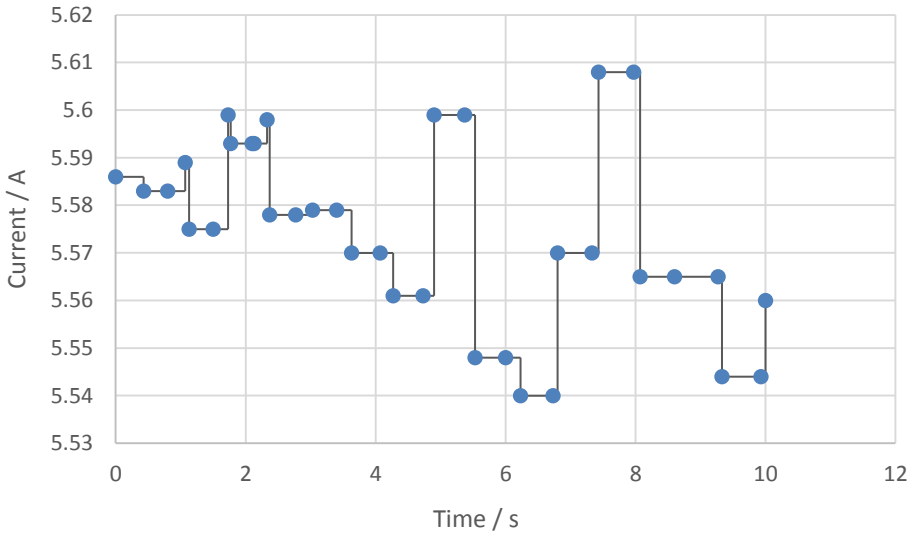

Figure 5-3. Current Provided by the Power Supply

According to Eq. (5.6), the average more power for this 10 s period is calculated and considered as the average power for the motor throughout the test because of its periodical characteristic. Using Microsoft Excel, the motor power P_{MOT} is obtained.

$$P_{MOT} \approx 22.03\ W \tag{5.7}$$

5.2.5. Transmission Roller Efficiency (η_t)

Using the method introduced in Chapter 4.1, the efficiency for the transmission roller in the prototype is calculated in this section using the data collected from testing.

In Chapter 4.1, the normal force that is applied by the track on the ball bearings F_p is expressed with a constant coefficient *A* in Eq. 4.7 and 4.8. This constant *A* could be calculated using Eq. 4.20 which is based on the fact that the average accelerating torque equals to the average decelerating torque for the revolver when the pump achieves a balanced and stable working status. Then the transmission efficiency η_t could be obtained through Eq. 4.23 using the data collected from the test.

The values for parameters in this prototype are rewritten here. $D_t = 2.65\ in, l = 0.8\ in, \mu = 0.35$. The coefficient of friction is between steel and ABS, in a sliding situation [53].

First, the value of constant *A* needs to be calculated. Composite Simpson's rule is used to estimate the integral term in *A*. Composite Simpson's Rule is written as following [54]: Suppose that the interval [a, b] is split up in n subintervals, with n an even number. Then, the composite Simpson's rule is given by

$$\int_a^b f(x)dx \approx \frac{h}{3}[f(x_0) + 4f(x_1) + 2f(x_2) + 4f(x_3) + 2f(x_4) + \cdots + 4f(x_{n-1}) + f(x_n)] \quad (5.8)$$

where $x_j = a + jh$ for $j = 0, 1, \cdots, n-1, n$; $h = (b-a)/n$.

In this case, the integral term is $\int_0^{\frac{\pi D_t}{8}} sin\left(\frac{4}{D_t}x\right)\frac{\mu - \dot{y}}{\sqrt{\dot{y}^2+1}}dx$, so $a = 0, b = \frac{\pi D_t}{8}, f(x) = sin\left(\frac{4}{D_t}x\right)\frac{\mu - \dot{y}(x)}{\sqrt{\dot{y}^2(x)+1}}$. n is chosen to be 4.

$$\int_0^{\frac{\pi D_t}{8}} sin\left(\frac{4}{D_t}x\right)\frac{\mu - \dot{y}}{\sqrt{\dot{y}^2+1}}dx \approx \frac{\pi D_t}{96}\left[f(0) + 4f\left(\frac{\pi D_t}{32}\right) + 2f\left(\frac{\pi D_t}{16}\right) + 4f\left(\frac{3\pi D_t}{32}\right) + f\left(\frac{\pi D_t}{8}\right)\right] = 0.0124\ m \quad (5.9)$$

The accuracy of this estimation depends on the choice of n. The larger its value, the more accurate is this estimation. Since integral term is also approximately equal to 0.0124 when n is chosen as 6, there is no need in making n bigger than 4 which needs more computing time.

According to Eq. 2.15 $\omega = \pi n$, the value of *A* is calculated as

$$A = \frac{\pi P_{mot}}{32\omega \int_0^{\frac{\pi D_t}{8}} sin\left(\frac{4}{D_t}x\right)\frac{\mu - \dot{y}}{\sqrt{\dot{y}^2+1}}dx} = \frac{\pi \times 22.03W}{32 \times 1.28\pi/s \times 0.0124m} = 43.37\ N \quad (5.10)$$

After the value of *A* is obtained, the energy loss could be calculated using Eq. 4.22. Again, composite Simpson's rule is used for estimation of the integral term where n is also chosen to be 4.

$$\int_0^{\frac{\pi D_t}{8}} sin\left(\frac{4}{D_t}x\right)\sqrt{1+\dot{y}^2}\,dx \approx \frac{\pi D_t}{96}\left[f(0)+4f\left(\frac{\pi D_t}{32}\right)+2f\left(\frac{\pi D_t}{16}\right)+4f\left(\frac{3\pi D_t}{32}\right)+ f\pi Dt8=0.0187\,m\right] \quad (5.11)$$

The value of n is still chosen as 4 since the integral estimation value still remains the same when n is chosen as 6 or bigger.

$$W_f = 16\mu A\int_0^{\frac{\pi D_t}{8}} sin\left(\frac{4}{D_t}x\right)\sqrt{1+\dot{y}^2}\,dx = 4.54\,J \quad (5.12)$$

It is obvious that $n=\frac{1}{T}$. According to Eq. 4.23, the transmission efficiency for the transmission roller could be obtained by

$$\eta_t = 1-\frac{W_f}{P_{mot}T} = 1-\frac{W_f n}{P_{mot}} = 73.6\% \quad (5.13)$$

5.2.6. Overall Efficiency (η)

The efficiency that is tested and calculated here is the overall efficiency for the pump prototype η. It is defined as the ratio of the pump output power and the motor power.

$$\eta = (P_W/P_{MOT})\times 100\% = (0.573/22.03)\times 100\% = 2.6\% \quad (5.14)$$

It is proved that the proposed transmission roller is fully functional as a power transmission device while keeping the pump design simple and compact.

Chapter 6.
Discussion and Analysis

From these tests, not only a better understanding about the pump prototype could be obtained, but also it could provide information to predict the performance of the final industrial design. For the prototype, its load force is first analyzed in order to understand its different operation conditions from the real production design. Different factors which cause its low prototype overall efficiency are analyzed as well. For the final production design, the transmission efficiency for the transmission roller is predicted using the method introduced before. To satisfy a specific flow rate requirement, various ways of adjusting the parameters of the design are illustrated.

6.1.1. Load Force in the Prototype

Load force directly applies on the transmission roller and thus analysis of this force is necessary in order to make sure that the transmission roller is able to withstand it. Eq. 4.30 is an expression of the load force F_{ld} through which a maximum of the load force could be obtained. Substitute Eq. 4.24 into Eq.4.30, it is obtained

$$F_{ld} = \frac{1}{4}\pi\rho D^2[L - \frac{l}{2}sin\left(2\omega t - \frac{\pi}{2}\right)] \times (g - 2l\omega^2\, sin(2\omega t - \frac{\pi}{2})) \tag{6.1}$$

In this prototype, $\rho = 1 \times 10^3\ kg/m^3$, $D = 3.25\ in$, $L = 4.6\ in$, $l = 0.8\ in$, $\omega = \pi n = 1.28\pi\ rad/s$. To obtain the maximum of the load force F_{ld}, the expression is transformed as below.

$$F_{ld} = \frac{1}{4}\pi\rho D^2\{l^2\omega^2\left[sin\left(2\omega t - \frac{\pi}{2}\right) - \left(\frac{L}{l} + \frac{g}{4lw^2}\right)\right]^2 - L^2\omega^2 + \frac{1}{2}Lg - \frac{g^2}{16w^2}\} \tag{6.2}$$

After substituting the values of the parameters into the equation, it is easy to find that the maximum of the load force is achieved when $sin\left(2\omega t - \frac{\pi}{2}\right) = -1$. In other

words, when the plunger of the transmission roller goes through its lowest point, the load force achieves its biggest value. The biggest load force for the pump prototype is given by

$$F_{ld} = 7.17\ N \tag{6.3}$$

This force is so small that it is obviously safe for the 3D printed transmission roller. However, this calculation only applies to the situation when the motor rotary speed is 1.28π rad/s or when the pumping speed is 1.28 cycle/s. In fact, the maximum load force changes when the pump speed n changes, as shown in Figure 6-1.

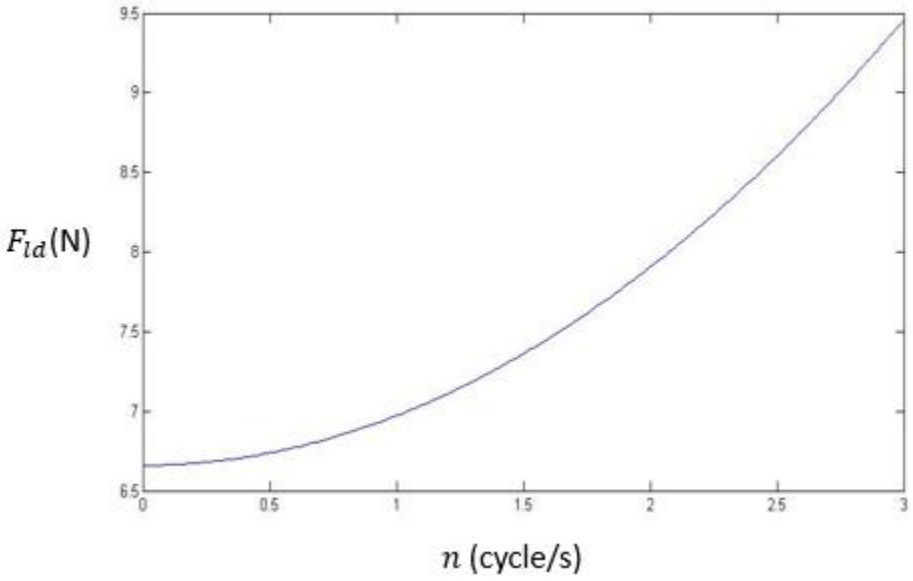

Figure 6-1. The Maximum of The Load Force VS Pump Speed

From the graph it could be observed that when the pump speed is 3 cycle/s, the maximum load force could rise up to $9.4\ N$. At the same time, the frequency that the check valves are working with is $3\ Hz$. If a type of check valves could be found which is able to work with higher frequency, the maximum load force would keep increasing as the pump speed increases. Note that all the values calculated are for the pump prototype built for this project. For the final industrial design, the loading force depends on the requirement for output pressure.

6.1.2. Transmission Roller Efficiency

The transmission roller efficiency of this prototype is 73.6% as calculated in Chap. 5. This is relatively low for a power transmission device and it is due to the high friction between the ball bearings and the tracks. For the final production design, the transmission roller would be machined from hard metal, possibly steel, instead of 3D printed using ABS. The ball bearings could also be made with steel. The friction coefficient between greased steel could be as low as 0.03 [55]. Given $\mu = 0.03$ and assuming the other parameters remain unchanged as in the test, the transmission efficiency for the transmission roller in the final production design could be calculated using the same method introduced in Chap. 4.

$$\int_0^{\frac{\pi D_t}{8}} sin\left(\frac{4}{D_t}x\right)\frac{\mu-\dot{y}}{\sqrt{\dot{y}^2+1}}dx \approx 0.0075m \tag{6.4}$$

$$A = \frac{\pi P_{mot}}{32\omega\int_0^{\frac{\pi D_t}{8}} sin\left(\frac{4}{D_t}x\right)\frac{\mu-\dot{y}}{\sqrt{\dot{y}^2+1}}dx} = 71.71\ N \tag{6.5}$$

$$W_f = 16\mu A\int_0^{\frac{\pi D_t}{8}} sin\left(\frac{4}{D_t}x\right)\sqrt{1+\dot{y}^2}\,dx = 0.644\ J \tag{6.6}$$

$$\eta_t = 1 - \frac{W_f}{P_{mot}T} = 1 - \frac{W_f n}{P_{mot}} = 96.3\% \tag{6.7}$$

For most conventional pumps with mechanical crankshafts or cam shafts, their plunger diameters usually have an impact on the mechanical efficiency. When plunger diameter is around 3.25", the mechanical efficiency for highly lubricated package is usually within the range from 78% to 91% [13]. Compared with those, the mechanism proposed in this thesis is highly promising in delivering a better performance in terms of mechanical efficiency.

6.1.3. Over Pump Efficiency

The overall pump efficiency for the prototype is calculated to be 2.6% in Chap.5. With the transmission roller efficiency being 73.6% in the prototype, there must be some

other factors that are much more energy-consuming than the transmission roller. Different factors which cause the low pump efficiency are being analysed in this section and how to avoid these energy losses for the final production design is discussed.

The major reason for the energy losses is friction between the U-cups around the plunger and the pump tube. The purpose of these seals is to contain water within the pump chamber and to prevent leakage into the motor area. The fact that these seals are necessary in the prototype is due to the absence of the diaphragm in the pump design. As mentioned in Chapter 2, the diaphragm is taken out to simplify the prototype building process. Though this modification doesn't get in the way of demonstrating the concept and the function of the transmission roller, it creates a chance for potential process fluid leakage. The sealing around the plunger needs to be tight enough to avoid the fluid leakage and protect the motor. At the same time, the sealing is always in dynamic motion in the same reciprocating manner as the plunger, without oil lubrication. This causes a big friction and also reduces the overall pump efficiency. For the final production design, this issue doesn't exist if the diaphragm is present. With the diaphragm and the oil layer outside the diaphragm, the sealing doesn't need to be as tight as in the prototype since both sides of the sealing are bathed in oil. Also the oil itself could function as a lubricator which reduces the friction.

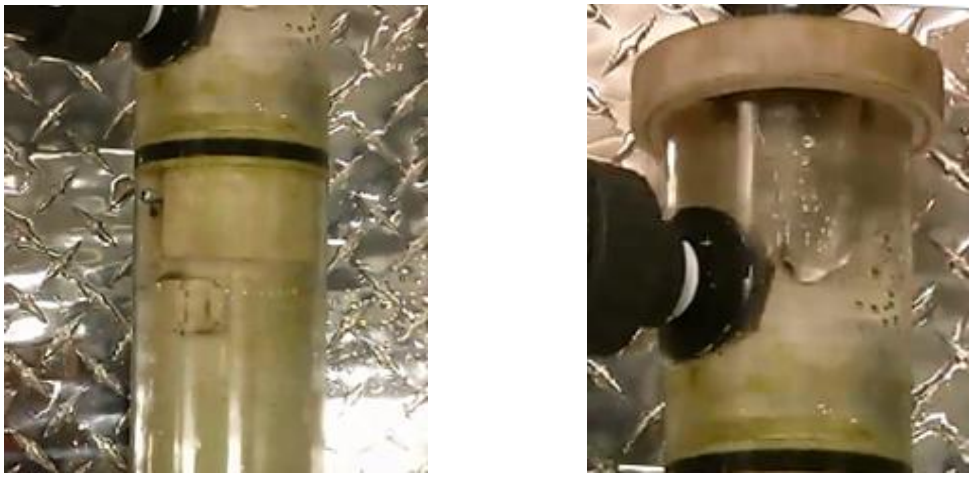

a) U-cup Seals b) Air Bubbles

Figure 6-2. Factors that Affect the Overall Pump Efficiency

Another factor that obviously causes some energy losses is the air leakage into the pump system. It could easily be observed through the experiment that the air is leaked into the pump chamber. With compressible air in the pump chamber, less fluid is pumped out by each stroke and thus the volumetric efficiency and the overall pump efficiency are reduced. The air is mainly leaked in through different tube fittings and pump connections both at the inlet and outlet. These connections are made mostly watertight through NPT threads and Teflon tape, but not airtight. For example, leakage or air bubbles could be observed at the connection between the inlet check valve and the pump tube. This air leakage wouldn't be an issue for the final production design because most of the connections would be welded and thus airtight. The transferred fluid would also be separated by the diaphragm which guarantees zero leakage.

Another minor factor which affects the overall pump efficiency is the unsmooth movement caused by the inaccuracy in the prototype modelling. Some parts are machined manually in the prototype and have accumulated errors when assembled. For example, inaccuracy in locating the holes on the pump tube for the side locks resulted in shocks and vibrations. This is because the side lock bearings keep bumping into other parts of the transmission roller. These vibrations and shocks won't exist if the holes are accurately drilled. These kinds of inaccuracies in machining add up and cause unnecessary vibrations which consume the energy from the pump.

6.1.4. Flow Rate

When used for real applications, usually there are different requirements for flow rate in different applications. In this section, it is introduced how to adjust the design for different requirements. Take the specifications from Toyo pumps as an example, the flow rate is required to be at least $50\ GPM$.

According to Eq. 3.1, the flow rate could be expressed as below

$$Q = \pi(\frac{D}{2})^2 ln = 50\ GPM \tag{6.8}$$

The parameters that affect the flow rate Q are the tube diameter D, the stroke length l and the pump speed n. The tube diameter which is equal to the diameter of the plunger of the transmission roller decides how big the pump body is going to be. Usually the tube diameter needs to be smaller than 3.5" for slurry applications and the requirements are different for different applications. The stroke length l is also the amplitude of the sine curved track on the transmission roller. It is limited by the diameter of the plunger because steep tracks are not desired. However, if a really large stroke length is desired, the design transmission roller II could be considered. The pump speed is decided by the motor power, but it is limited by the frequency of the check valves. Mechanical check valves usually have a limitation for the frequency that they could work with. The pump speed cannot exceed the frequency limit of the check valves.

With different pump speeds, different combinations of stroke length l and tube diameter D that satisfy the flow rate requirement are shown in Figure 6-3. Different design points are shown for pump speed 1 cycle/s, 2 cycle/s and 3 cycle/s separately. The stroke length is from 0.26" to 23.20". The tube diameter is from 3.25" to 17.5".

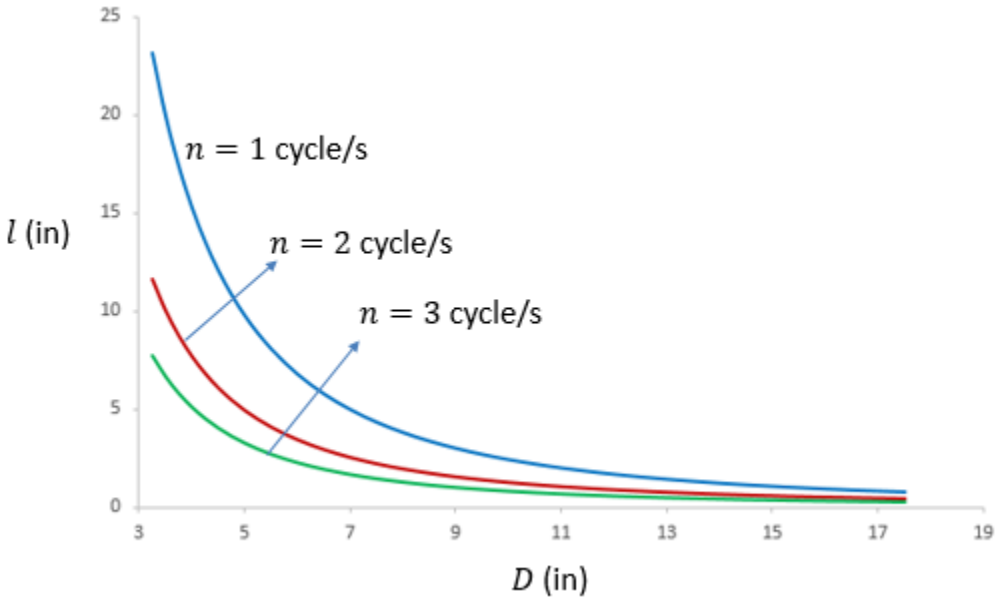

Figure 6-3. Design Points for Flow Rate 50 GPM

It could be observed that with a certain tube diameter, a smaller stroke length is needed for a pump with larger speed to achieve the same flow rate. With a certain pump

speed, the bigger the tube diameter is, the smaller the stroke length needs to be to achieve the same flow rate. From Figure 6-3, it could be observed that when the pump speed is 3 cycle/s, the design point which has a track of the same steepness as the prototype is of 7” tube diameter and 1.7” stroke length, to achieve 50 GPM flow rate.

Unlike centrifugal pumps, positive displacement pumps (PDPs) force the fluid along by volume changes. Resistance to the flow of fluid is produced by downstream process or piping system, thereby pressure is generated in the piping system and in the discharge portion of the pump. Therefore, flow rate does not have direct impact on the output pressure of pump design, nor does the diameter of the pump tube. The factors that influence the head pressure of the production pump design include the motor power and the resistance to the flow caused by downstream system, such as the cracking pressure of the check valves. The estimation of motor power for different head pressure requirements is discussed in the following section.

6.1.5. Motor Power

Usually the head pressure requirement could vary from 0 to 1000 psi for slurry applications. For the proposed pump design, motors with different power ratings should be chosen to achieve different head pressure requirements. Assuming the efficiency of the pump is 100%, an estimation of the minimum power needed to actuate the pump based on its head pressure and flow rate requirement is presented in this section.

Based on Eq. 5.3 and 5.5, the motor power output is given by

$$P_W = Q \times p_H \approx p_{out} Q \tag{6.9}$$

Based on the above equation, the power output required is estimated as shown in Figure 6-4, in which the head pressure ranges from 200 to 1000 psi and the flow rate is 50 GPM, 150 GPM or 450 GPM.

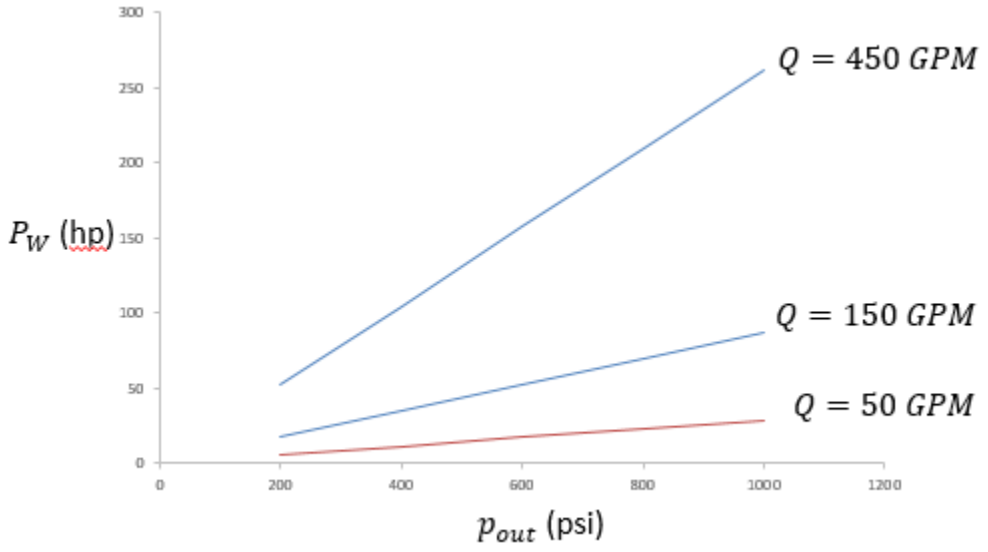

Figure 6-4. Estimated Power Output for Different Requirements

However, when choosing a motor for the production design pump, two more factors need to be considered. Firstly, the pump efficiency will not be 100% and the energy losses should be considered when trying to set the expected power output from the motor. Secondly, the efficiency of the motor should also be considered which is usually stated in the specifications of a motor.

Chapter 7.
Conclusions and Recommendations

The oil and gas industry needs a simple and compact pump design that can deal with slurry and other highly viscous or erosive fluid. The design needs to fit in a borehole and perform with a comparable or higher efficiency than the current pumps used in similar situations. Diaphragm pumps are often used in slurry applications dealing with corrosive and erosive fluid. They are good at handling fluid with high viscosity, which is an advantage for most reciprocating pumps. Another advantage of a diaphragm pump is that it maintains a constant flow rate regardless of pressure, thereby tending to “purge” any plugging effect. The fact that most pump components are protected from the transferred fluid by the diaphragm gives a diaphragm pump good sealing performance and a longer lifetime. Thus, diaphragm pump is chosen as the basic model for this design. However, the traditional power transmission system for a diaphragm pump is bulky and has a low efficiency, which needs to be modified and improved for this application.

Using smart material in the pump actuation system is considered to achieve a compact pump design, similar to a peristaltic pump. Piezoelectric material is chosen as the most promising candidate for its capability to generate high forces and to work under high frequencies. However, a conclusion is drawn after a preliminary analysis that it is not powerful enough to actuate a pump of the size in slurry applications. Inspired by algebraic screw used in vehicle suspension systems, another solution is proposed to achieve a compact design. Transmission Roller I is designed to be used as a power transmission device in the pump design. It could convert rotary motion into linear motion and rotate continuously without direction change. It is also very promising to have a high efficiency with a much slimmer structure compared to traditional sliding cranks or gear transmissions. Transmission Roller II could be seen as an extended design for Transmission Roller I. By using a bearing group, the rolling direction of the bearing group

at the track intersections are controlled so that the stroke length of the mechanism could be lengthened. However, Transmission Roller II has more complicated structure than Transmission Roller I and thus worse structure integrity than Transmission Roller I.

A pump prototype utilizing the proposed transmission roller is built. Major parts of the transmission roller are 3D printed with ABS while other parts in the prototype are machined with steel or purchased from the market. Diaphragm is taken away from this prototype design to simplify the building process. The purpose of building the prototype is to validate the functionality of the proposed transmission roller. The prototype is tested with water. It is observed that the prototype is working fine and the transmission roller is functioning well as expected.

From the test, it is deduced that the capacity of the pump prototype is 2.665 GPM when the pump speed is 1.28 cycle/s. The transmission roller efficiency for the prototype is 73.6%. Based on the mathematical model built and the experimental data, the transmission roller efficiency for the final production design would be 96.3%.

7.1. Recommendation for future work

For the prototype, a diaphragm could be added to improve the overall efficiency. With the diaphragm present, the seals around the plunger don't need to be as tight and are lubricated by oil. The diaphragm would also separate the transferred fluid from the outside and thus generate a leakage free environment. It also prevents air leaked into the system and compromise the volumetric efficiency. The tube fittings could also be improved by choosing the ones which are more airtight.

For the final industrial production design, Transmission Roller II could be considered to extend the stroke length. The structural integrity of its bearing group should be examined, especially for high output pressure applications. The process of examining structural integrity could be the same as analyzing Transmission Roller I using ANSYS. In this case, instead of 3D printing with ABS, the transmission roller analyzed is made of stainless steel, which is more likely to be the case in industrial productions. The results show that it is necessary to strengthen the structure of the

transmission roller when the output pressure requirement for the application is 1000 psi. It could be done by increasing contact areas or plate thicknesses. Also it could be done by upgrading the building material to a stronger one. After modification, the safety factors for the model should be above 1. Tests could be run on this metal prototype to measure the efficiency of this mechanism.

References

[1] Warman International LTD., “Slurry Pumping Manual,” 2002.

[2] LaBour Pump Company, “Pump Wear,” 2005.

[3] J. Gamboa, J. Iglesias, and P. Gonzalez, “Understanding the Performance of a Progressive Cavity Pump with a Metallic Stator,” *Proc. Twenty-Fifth Int. Pump Users Symp.*, 2003.

[4] “Borehole.” [Online]. Available: http://en.wikipedia.org/wiki/Borehole.

[5] P. Cooper, “A Vision And Mission For Pump R & D Over The Next 25 Years,” *Proc. Twenty-FifthInternational Pump Users Symp.*, 2009.

[6] D. Hartog, “Mechanical Vibrations in Penstocks of Hydraulic Turbine Installations,” *Trans. ASME*, 1929.

[7] Fisher and Thomas, “Investigation of the Flow Conditions in a Centrifugal Pump,” *Trans. ASME*, vol. 54, 1932.

[8] R. T. KNAPP, A.Hollander, Pasadena, and Calif, “Laboratory Investigations of the Mechanism of Cavitation,” *Trans. ASME*, 1948.

[9] C. Blom, “Development of the Hydraulic Design for the Grand Coulee Pumps,” *Trans. ASME*, 1950.

[10] H. Stahl, A. Stepanoff, and N. Phillipsburg, “Thermodynamic Aspects of Cavitation in Centrifugal Pumps,” *ASME J. Basic Eng*, 1956.

[11] R. FURST, “SPACE SHUTTLE MAIN ENGINE TURBOPUMP DESIGN,” *SAE Tech. Pap.*, 1973.

[12] Frank M. White, *Fluid Mechanics*, 4th ed. Singapore: McGraw-Hill Book Co-Singapore, 1999.

[13] T. L. Henshaw, *Reciprocating Pumps*. New York: Van Nostrand Reinhold Company Inc., 1987.

[14] Ingersoll-Rand, *Ingenious Mechanisms*. New York, 1960.

[15] Hohn E. Miller, *The Reciprocating Pump*. USA: Wiley-Interscience, 1987.

[16] A. W. Ruff, *Tribology: Wear Test Selection for Design and Application*. Baltimore, 1993.

[17] I. J. Karassik, J. P. Messina, and W. H. Fraser, *Pump Handbook*. 1986.

[18] C. A. Keller, "Novel Concepts In Piezohydraulic Pump Design," *Thesis Submitt. to Georg. Inst. Technol.*, 2004.

[19] D. Berlincourt, "Piezoelectric Ceramics Characteristics and Applications," *J. Acoust. Soc. Am.*, 1980.

[20] H. Tan, D. J. Leo, H. H. Robertshaw, and C. L. Dancey, "Performance Modeling and Efficiency Analysis for a Piezohydraulic Pump with Active Valves," *Thesis Submitt. to Fac. Virginia Polytech. Inst. State Univ.*, 2002.

[21] H. Haertling, "Rainbow Actuators and Sensors: A New Smart Technology," in *Proc. SPIE Conf.*, 1997.

[22] M. Mossi and P. Bishop, "Characterization of Different Types of High Performance Thunder Actuator," in *Proc. SPIE Conf.*, 1999.

[23] K. M. Mossi, G. V. Selby, and R. G. Bryant, "Thin-Layer Composite Unimorph Ferroelectric Driver Sensor Properties," no. April, pp. 39–49, 1998.

[24] D. J. Laser and J. G. Santiago, "A Review of Micropumps," *J. Micromechanics Microengineering*, vol. 14, pp. R35–R64, 2004.

[25] T. Gerlach and H. Wurmus, "Working Principle and Performance of the Dynamic Micropump," *Proc. IEEE Micro Electro Mech. Syst.*, 1995.

[26] J.-H. Park, K. Yoshida, and S. Yokota, "Resonantly Driven Piezoelectric Micropump," *Mechatronics*, vol. 9, pp. 687–702, 1999.

[27] L. D. Mauck and C. S. Lynch, "Piezoelectric Hydraulic Pump Development," *J. Intell. Mater. Syst. Struct.*, vol. 11, no. 10, pp. 758–764, Oct. 2000.

[28] K. Konishi, T. Yoshimura, K. Hashimoto, and N. Yamanoto, "Hydraulic Actuators Driven by Piezoelectric Elements (1st Report, Trial Piezoelectric Pump and Its Maximum Power)," *Biosci. Biotechnol. Biochem.*, 1993.

[29] J. D. Robinson, M. J. D. Hayes, D. D. Une, and P. Alge, "The Dynamics of A Single Algebraic Screw Pair," vol. 35, no. 4, pp. 491–503, 2011.

[30] J. Griffis, M. and Duffy, “Method and apparatus for controlling geometrically simple parallel mechanisms with distinctive connections,” 1993.

[31] R. Sabzehgar, A. Maravandi, and M. Moallem, “Energy Regenerative Suspension Using an Algebraic,” *IEEE/ASME Trans. MECHATRONICS*, pp. 1–9, 2013.

[32] M. L. Husty and A. Karger, “Self-Motions of Griffis-DuEy Type Parallel Manipulators,” *Proc. 2000 IEEE Int. Conf. Robot. Autom.*, no. April, pp. 7–12, 2000.

[33] J. John J.Uicker, G. R. Pennock, and J. E.Shigley, *Theory of Machines and Mechanisms*, 4th ed. New York: Oxford University Press, 2011.

[34] Hidalgo-Martinez, “Design of cams with negative radius follower using Bezier curves,” *Mech Mach Theory*, 2014.

[35] V. T. Nguyen and D. J. Kim, “Flexible cam profile synthesis method using smoothing spline curves,” *Mech. Mach. Theory*, vol. 42, pp. 825–838, 2007.

[36] Yong, “Research of cylindrical cam with oscillating follower 3D spread,” *Trans Chin Soc Agric Mach*, 2007.

[37] Physik Instrumente, “Forces and Stiffnesses,” *Physik Instrumente*. [Online]. Available: http://piceramic.com/piezo-technology/properties-piezo-actuators/forces-stiffnesses.html.

[38] “Stiffness.” [Online]. Available: http://en.wikipedia.org/wiki/Stiffness.

[39] K. T. Ooi, “Simulation of A Piezo-Compressor,” *Appl. Therm. Eng.*, vol. 24, pp. 549–562, 2004.

[40] Physik Instrumente, “Dynamic Operation.” [Online]. Available: http://piceramic.com/piezo-technology/properties-piezo-actuators/dynamic-operation.html.

[41] Mcmaster-Carr, “Steel Ball Bearing.” [Online]. Available: http://www.mcmaster.com/#6383k12/=xh9yt1.

[42] H. H. Tackett, J. A. Cripe, and G. Dyson, “Positive Displacement Reciprocating Pump Fundamentals-Power and Direct Acting Types,” *Proc. Twenty-Fourth Int. Pump Users Symp.*, 2008.

[43] Mcmaster-Carr, “Lubrication-Free Acetal Ball Bearing.” [Online]. Available: http://www.mcmaster.com/#6455k7/=xhat28.

[44] Sealsonline, “8400 Nitrile NBR80A.” [Online]. Available: http://sealsonline.com/website/catalog_list.asp?cat=Rod-Piston+Seals&code=130071&CatgName=8400.

[45] Maxon Motor, “Maxon A-max Motor 236668.” [Online]. Available: http://www.maxonmotor.com/maxon/view/product/motor/dcmotor/amax/amax32/236668.

[46] Maxon Motor, “Planetary Gearhead GP 32 C.” [Online]. Available: http://www.maxonmotor.com/maxon/view/product/gear/planetary/gp32/166931.

[47] Mcmaster-Carr, “Light Duty Plastic Turntable.” [Online]. Available: http://www.mcmaster.com/#1413t11/=xhsi6l.

[48] B. M. Fadhel, “Numerically Study of Ballistic Impact of Polycarbonate,” *SHUSER 2011 - 2011 Int. Symp. Humanit. Sci. Eng. Res.*, pp. 101–105, 2011.

[49] A. R. Book, *Machinery ’ s Handbook*, 28th ed. New York: Industrial Press.

[50] T. S. Lee, H. T. Low, D. T. Nguyen, and W. R. a Neo, “Experimental Study Of Check Valves Performances In Fluid Transient,” *Proc. Inst. Mech. Eng. Part E J. Process Mech. Eng.*, vol. 223, no. 2, pp. 61–69, May 2009.

[51] N. D. Manring, *Hydraulic Control Systems*. USA: John Wiley & Son Inc., 2005.

[52] American National Standard Institution, “Reciprocating Pump Tests.” 1994.

[53] Mechguru, “Typical Coefficient of Friction Values for Common Materials.” [Online]. Available: http://blog.mechguru.com/machine-design/typical-coefficient-of-friction-values-for-common-materials/.

[54] “Simpson’s Rule.” [Online]. Available: http://en.wikipedia.org/wiki/Simpson%27s_rule.

[55] “Coefficient of Friction Values for Greased Surfaces.” [Online]. Available: http://www.school-for-champions.com/science/friction_coefficient_greased.htm#.VVknlPlViko.

Appendix A.

PI Piezoelectric Actuators

This is a table for piezoelectric actuators provided by Physik Instrumente. These products are used as a technical bar to measure the limitations of piezoelectric actuators' performances available in the market.

Table A1 Specifications for PI Piezoelectric Actuators

Ordering Number	Displacement [µm -10/+20%]	Diameter D [mm]	Length L [mm ±0.5]	Blocking force [N]	Stiffness [N/µm]	Capacitance [nF ±20%]	Unloaded Resonant Frequency [kHz]
P-007.00	5	7	8	650	130	11	126
P-007.10	15	7	17	850	59	33	59
P-007.20	30	7	29	1000	35	64	36
P-007.40	60	7	54	1150	19	130	20
P-010.00	5	10	8	1400	270	21	125
P-010.10	15	10	17	1800	120	64	59
P-010.20	30	10	30	2100	71	130	35
P-010.40	60	10	56	2200	38	260	20
P-010.80	120	10	107	2400	20	510	10
P-016,10	15	16	17	4600	320	180	59
P-018,20	30	16	29	5500	190	340	36
P-016.40	60	16	54	6000	100	680	20
P-016.80	120	16	101	6500	54	1300	11
P-016.90	180	16	150	6500	36	2000	7
P-025.10	15	25	18	11000	740	400	56
P-025.20	30	25	30	13000	440	820	35
P-025.40	60	25	53	15000	250	1700	21
P-025.80	120	25	101	16000	130	3400	11
P-025.90	180	25	149	16000	89	5100	7
P-025.150	250	25	204	16000	65	7100	5
P-025.200	300	25	244	16000	54	8500	5
P-035.10	15	35	20	20000	1300	830	51
P-035.20	30	35	32	24000	810	1700	33
P-035.40	60	35	57	28000	460	3400	19
P-035.80	120	35	104	30000	250	6900	11
P-035.90	180	35	153	31000	170	10000	7
P-045.20	30	45	33	39000	1300	2800	32
P-045.40	60	45	58	44000	740	5700	19
P-045.80	120	45	105	49000	410	11000	10
P-045.90	180	45	154	50000	280	17000	7
P-050.20	30	50	33	48000	1600	3400	32
P-050.40	60	50	58	55000	910	7000	19
P-050.80	120	50	105	60000	500	14000	10
P-050.90	180	50	154	61000	340	22000	7
P-056.20	30	56	33	60000	2000	4300	32
P-056.40	60	56	58	66000	1100	8900	19
P-056.80	120	56	105	76000	630	18000	10
P-056.90	180	56	154	78000	430	27000	7

Appendix B.

Test Data on Voltage and Current

This is data collected during the 10 s sample of the water test, from the readings on the power supply. As illustrated in Chapter 5, voltage and current data keep changing during this period. The changes are recorded in the table below.

Table B1 Collected Data on Voltage and Current

Time/s	Voltage/V	Current/A	Time/s	Voltage/V	Current/A
0	4.24	5.586	4.27	4.38	5.561
0.43	4.24	5.583	4.73	5.06	5.561
0.8	5.26	5.583	4.9	5.06	5.599
1.07	5.26	5.589	5.37	5.32	5.599
1.13	5.26	5.575	5.53	5.32	5.548
1.5	4.75	5.575	6	4.98	5.548
1.73	4.75	5.599	6.23	4.98	5.54
1.77	4.75	5.593	6.73	4.36	5.54
2.1	4.99	5.593	6.8	4.36	5.57
2.13	4.51	5.593	7.33	5.15	5.57
2.33	4.51	5.598	7.43	5.15	5.608
2.37	4.51	5.578	7.97	5.17	5.608
2.77	6.54	5.578	8.07	5.17	5.565
3.03	6.54	5.579	8.6	4.94	5.565
3.4	5.02	5.579	9.27	5.05	5.565
3.63	5.02	5.57	9.33	5.05	5.544
4.07	4.38	5.57	9.93	4.93	5.544
			10	4.94	5.56